Molecular Therapy
Original Article

Highly Efficient Gene Editing of Cystic Fibrosis Patient-Derived Airway Basal Cells Results in Functional CFTR Correction

Shingo Suzuki,[1,6] Ana M. Crane,[1,6] Varada Anirudhan,[1,6] Cristina Barillà,[1] Nadine Matthias,[1] Scott H. Randell,[2] Andras Rab,[3] Eric J. Sorscher,[3] Jenny L. Kerschner,[4] Shiyi Yin,[4] Ann Harris,[4] Matthew Mendel,[5] Kenneth Kim,[5] Lei Zhang,[5] Anthony Conway,[5] and Brian R. Davis[1]

[1]Institute of Molecular Medicine, University of Texas Health Science Center at Houston, Houston, TX 77030, USA; [2]Department of Cell Biology and Physiology, The University of North Carolina at Chapel Hill, Chapel Hill, NC 27599, USA; [3]Department of Pediatrics, Emory University School of Medicine, Atlanta, GA 30322, USA; [4]Department of Genetics and Genome Sciences, Case Western Reserve University, Cleveland, OH 44106, USA; [5]Sangamo Therapeutics, Richmond, CA 94804, USA

There is a strong rationale to consider future cell therapeutic approaches for cystic fibrosis (CF) in which autologous proximal airway basal stem cells, corrected for *CFTR* mutations, are transplanted into the patient's lungs. We assessed the possibility of editing the *CFTR* locus in these cells using zinc-finger nucleases and have pursued two approaches. The first, mutation-specific correction, is a footprint-free method replacing the *CFTR* mutation with corrected sequences. We have applied this approach for correction of ΔF508, demonstrating restoration of mature CFTR protein and function in air-liquid interface cultures established from bulk edited basal cells. The second is targeting integration of a partial *CFTR* cDNA within an intron of the endogenous *CFTR* gene, providing correction for all *CFTR* mutations downstream of the integration and exploiting the native *CFTR* promoter and chromatin architecture for physiologically relevant expression. Without selection, we observed highly efficient, site-specific targeted integration in basal cells carrying various *CFTR* mutations and demonstrated restored CFTR function at therapeutically relevant levels. Significantly, Omni-ATAC-seq analysis revealed minimal impact on the positions of open chromatin within the native *CFTR* locus. These results demonstrate efficient functional correction of CFTR and provide a platform for further *ex vivo* and *in vivo* editing.

INTRODUCTION

There is still much to be learned about turnover of cells in the human airway, as well as the identity of potential stem/progenitor cells responsible for overall pulmonary architecture and maintenance. There is an emerging consensus, however, that pseudo-stratified epithelial tissue of the human proximal airway contains basal cells capable both of self-renewing cell division, as well as differentiation to other specialized cells, including ciliated and secretory cells. As such, proximal airway basal cells serve as a major class of stem/progenitor cells within the proximal airway.[1–4] Thus, there is strong rationale to consider future cell therapeutic approaches for CF in which autologous proximal airway basal cells, corrected for *CFTR* gene mutations, are transplanted into the lungs of affected CF patients. To that end, our objective has been to prepare a population of *CFTR* corrected, patient-specific airway basal cells, which retain the ability to develop pseudo-stratified airway epithelium with restored CFTR function. Several groups, including our own, have utilized various methods to directly correct or compensate for *CFTR* mutations in relevant cell types via editing or gene transfer.[5–21]

There is currently uncertainty about the relative contribution of different cell types to overall CFTR activity in the airway epithelium. Does the rare ionocyte population expressing high levels of CFTR dominate[22,23] or do other more abundant luminal cell types (secretory or ciliated), which apparently express CFTR at lower levels per cell, also contribute?[24] Importantly, the aforementioned cell types are derived from airway basal stem cells, which justifies our editing focus.[2,3,22]

It is important to consider frequencies at which cells in the CF airway would need to be corrected, either as a consequence of transplantation of edited airway basal cells or direct *in vivo* editing, for therapeutic benefit. Johnson et al.[25] reported that as few as 6%–10% corrected cells was sufficient to restore CF chloride ion transport levels to normal. A second study showed that 5% of pseudostratified epithelial cells expressing *CFTR* corrected the CF chloride transport defect.[26] However, these two studies used highly efficient viral vector promoters to express CFTR and therefore it cannot be

Received 18 October 2019; accepted 23 April 2020;
https://doi.org/10.1016/j.ymthe.2020.04.021.

[6]These authors contributed equally to this work.

Correspondence: Brian R. Davis, Institute of Molecular Medicine, University of Texas Health Science Center at Houston, Houston, TX 77030, USA.
E-mail: brian.r.davis@uth.tmc.edu
Correspondence: Anthony Conway, Sangamo Therapeutics, Richmond, CA 94804, USA.
E-mail: aconway@sangamo.com

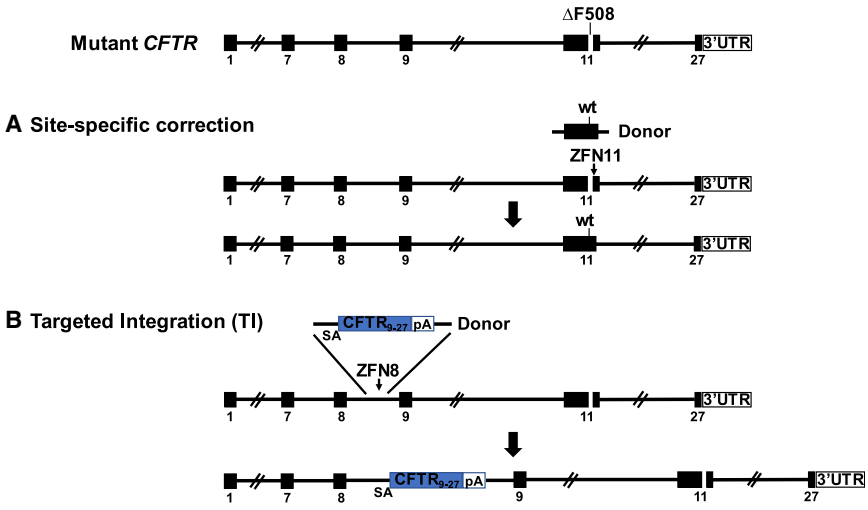

Figure 1. Site-Specific Editing of CF Airway Basal Cells

(A) Site-specific correction of ΔF508 mediated by targeted nuclease cleavage with wild-type DNA template serving as donor. (B) Integration of $CFTR_{9\text{-}27}$ cDNA (encoding exons 9–27), preceded by a splice acceptor (*SA*), followed by polyadenylation (*pA*) sequences, and flanked by homology sequences, into *CFTR* intron 8; the spliced mRNA joins endogenous exon 8 with the exon 9–27 transgene.

assured that comparable results would be obtained in differentiated human airway epithelia where *CFTR* is under the control of its endogenous promoter. In mixing experiments of human airway cells in air-liquid interface (ALI) cultures, it was reported that 20% of non-CF cells mixed into a background of 80% ΔF508/ΔF508 cells yielded CFTR chloride current at levels 70% of wild-type levels.[27] These data supported the concept that even a small fraction of cells expressing CFTR from the endogenous *CFTR* locus would be sufficient to correct the chloride transport defect in CF cells.[27]

The two approaches for *CFTR* gene editing in CF airway basal cells pursued by this study are shown in Figure 1. Our rationale for performing gene editing specifically of the endogenous *CFTR* locus reflects an intent to achieve expression of the corrected *CFTR* gene at close to physiologic levels. The first approach is site-specific correction of *CFTR* mutations; namely, a footprint-free method replacing mutant *CFTR* sequences with the corrected sequences (Figure 1A). Because CF is a recessive disease, correction of only one *CFTR* allele per cell would be sufficient for rescue of CFTR function. Site-specific correction of *CFTR* mutations in the endogenous gene is expected to result in physiologically appropriate levels of CFTR protein and function. However, site-specific correction typically requires a distinct set of sequence-directed nuclease and oligonucleotide donor reagents for each *CFTR* mutation. Because approximately 2,000 different CF-associated mutations have been reported, the sequence-specific approach would only seem justified for the most frequently occurring variants such as ΔF508. The second approach is homologous recombination-mediated targeted integration (TI) of a codon optimized partial *CFTR* cDNA (also denoted as a "super-exon")[5,7] preceded by a splice acceptor (SA) and followed by a polyadenylation (pA) sequence, within an intron of the endogenous *CFTR* gene (Figure 1B). This approach is capable of providing correction for all *CFTR* mutations downstream of the targeted partial *CFTR* cDNA integration site. Furthermore, by targeting cleavage of the genomic DNA within intronic versus exonic sequences, the possibility that nuclease-induced indels will adversely impact uncorrected alleles is minimized. With the objective of achieving physiologically regulated levels of CFTR expression and function, this approach would also benefit, in principle, from endogenous *CFTR* promoter activity and native chromatin architecture, provided that TI of the partial *CFTR* cDNA does not disrupt chromatin architecture in edited cells.

RESULTS

Feeder-free Expansion of Primary Airway Basal Cells with Retention of CFTR Function

Starting with early passage primary human airway epithelial cells from explanted CF or non-CF lungs, we first compared feeder-free culture methodologies for their ability to expand airway basal cells for numerous passages while retaining functional capability. Both the previously reported dual SMAD inhibition medium[28] and Pneumacult Ex-Plus medium allowed for continuous proliferation to at least passage 12 (p12; corresponding to 35–37 population doublings [PDs]; Figure S1A) while retaining markers characteristic of basal cells (e.g., CD49f, NGFR; Figure S1B). In order to assay functionality, expanded cells at various passage numbers were plated onto porous membranes and subject to ALI culture to assess development of well-differentiated airway epithelium. With increasing passage number, particularly for the dual SMAD inhibition culture, we noted progressive loss of ciliated cells, as measured by acetylated tubulin (Figure S1C). In order to measure CFTR ion transport function, ALI cultures were subjected to Ussing chamber assays. Airway basal cells expanded under Pneumacult Ex-Plus culture conditions exhibited robust levels of CFTR function through at least p8, while basal cells expanded in dual SMAD cultures exhibited lower levels of activity (Figures S1D and S1E). Under either culture condition, further passaging beyond p8 resulted in decreased levels of CFTR-dependent transepithelial transport (Figure S1E). Based on the above, we chose to perform our gene-editing manipulations on airway basal cells maintained maximally until p6 to p8 (~18–25 PDs) in the Pneumacult Ex-Plus medium.

Sequence-Specific Correction of ΔF508 Mutation

Zinc-finger nucleases (ZFNs), targeted to recognize and cleave *CFTR* ΔF508 sequences in exon 11 (ZFN11; Figure S2A), were delivered as mRNA to ΔF508/ΔF508 airway basal cells via electroporation. For

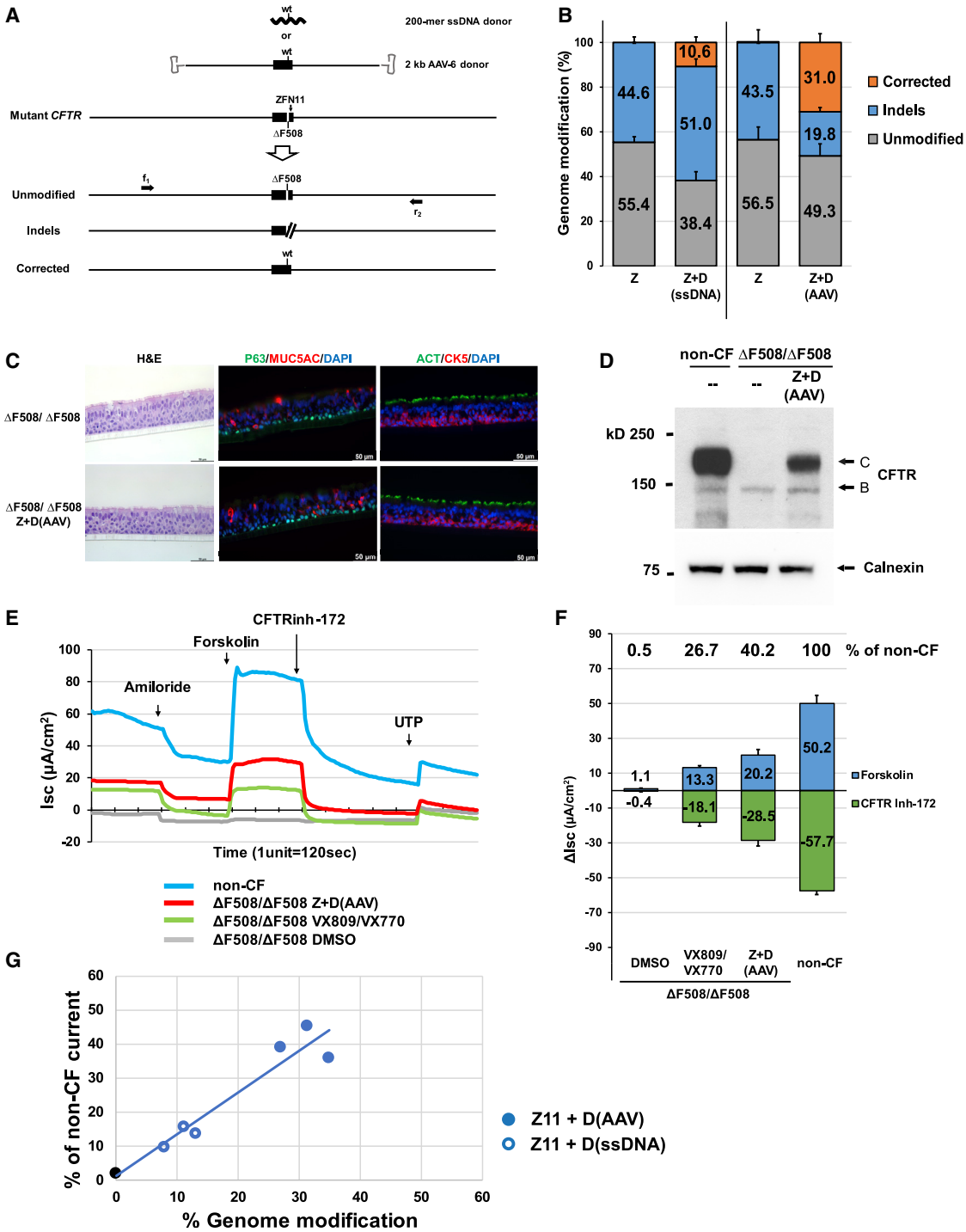

Figure 2. Sequence-Specific ΔF508 Correction with Restoration of Mature CFTR Protein Expression and Function

(A) Schematic of sequence-specific ΔF508 correction strategy. ZFNs were designed to site-specifically recognize and cleave *CFTR* ΔF508 sequences in exon 11 (ZFN11). Two donors carrying correcting *CFTR* sequence are shown: a single stranded 200-mer oligo DNA donor (ssDNA) and 2 kb AAV-6 donor (containing 1,963 bp of wild-type *CFTR* sequence spanning exon 11). Three anticipated outcomes are represented as unmodified, indels, and corrected. Primers f_1 and r_2, located outside the 1,963 bp donor sequence, were used to amplify the targeted region in order to assess genome modification efficiency. (B) Efficiency of genome modification analyzed by NGS. Z, ZFN11 alone; Z+D, ZFN11 plus donor DNA (mean ± SD, n = 3 biological replicates; see also Table S1). (C) H&E staining and immunofluorescence detection of airway epithelium markers in ALI culture. Major epithelial cell types were identified with markers: p63 or keratin 5 (CK5) for basal cells; mucin 5AC (MUC5AC) for secretory cells; acetylated

(legend continued on next page)

correction of the ΔF508 mutation, we evaluated two types of donor sequences encoding wild-type *CFTR* sequence. First, we co-delivered single-stranded (ss) 200-mer oligo DNAs together with the ZFN mRNAs via electroporation (Figure 2A). The ss oligo, centered on the ΔF508 mutation, included the wild-type restoring "CTT" bases (Figure S2A) spanned by approximately 100 bases of homology sequence on either side. In order to achieve maximal levels of correction while retaining cell viability, optimization was performed with respect to amount of ZFN mRNA (data not shown) and ssDNA donor oligo (e.g., Figures S2B and S2C). Next generation sequencing (NGS) was utilized to quantify the frequency of ΔF508 *CFTR* alleles exhibiting either no modification, indels, or correction (Figures 2A and 2B, Table S1). Delivery of ZFN mRNA alone resulted in 44.6% ± 2.4% of *CFTR* alleles exhibiting indels. When ssDNA donor was co-delivered with ZFN mRNA, the frequency of ΔF508 correction was 10.6% ± 2.6% (all editing frequencies are expressed on a per *CFTR* allele basis) (Figure 2B; Table S1). We sought to modify our methodology in order to achieve significantly higher efficiencies of correction. To this end, we utilized a longer donor (~2.0 kb, again centered on the correcting "CTT" bases), but in this case delivered via adeno-associated virus type 6 (AAV-6) (Figure 2A); AAV-6 was selected due to its favorable tropism for the lung.[29,30] Optimization was again performed, in this case focused on the amount of ZFN and the AAV-6 dose (Figure S2D). Delivery of ZFN mRNA via electroporation followed immediately thereafter by AAV-6 donor transduction resulted in a correction efficiency of 31.0% ± 4.0% (Figure 2B; Table S1).

Sequence-Specific ΔF508 Correction Restores Mature CFTR Protein Expression and Function

In order to assess the functional consequences of ΔF508 correction, cells edited with the 2 kb AAV-6 donor were transferred onto porous supports and subjected to ALI culture conditions to generate well-differentiated airway epithelium containing basal cells (p63, keratin 5), secretory cells (mucin 5AC), ciliated cells (acetylated tubulin, FOXJ1), and ionocytes (FOXI1; Figures 2C and S3). Importantly, the manipulations required for editing did not alter the development of the pseudostratified epithelium. For example, cellular composition of the derived epithelium (i.e., % basal cells, % secretory cells, % ciliated cells, % ionocytes) was not affected by the manipulations (Figure S3).

As expected, ALI cultures derived from unmanipulated ΔF508/ΔF508 airway basal cells only expressed the core glycosylated CFTR protein (band B; Figure 2D), whereas non-CF ALI cultures primarily exhibited the mature, fully-glycosylated, membrane-bound form of CFTR (band C; Figure 2D). Importantly, the AAV-6 edited ΔF508/ΔF508 cultures demonstrated the emergence of band C, corresponding to the presence of corrected *CFTR* alleles in the treated cells (Figures 2D and S4). Electrophysiological measurement of CFTR channel function was performed via Ussing chamber analysis. In Figure 2E, tracings for a representative experiment are presented; results of several experiments are presented in Table S2A and summarized in Figure 2F and Table S2B. As expected, non-treated ΔF508/ΔF508 cultures exhibit negligible forskolin-activated CFTR current (Figure 2F). ALI cultures derived from ΔF508/ΔF508 cells treated with ZFNs plus AAV-6 donor exhibited CFTR-dependent current (20.2 ± 3.5 μA/cm^2 (Figure 2F), robustly blocked by the CFTR channel inhibitor (CFTRinh-172; Figures 2E and 2F). This level of restored CFTR activity in edited cultures is significant in two respects. First, this level of rescue in bulk-treated ΔF508/ΔF508 cultures (with a mean correction efficiency of 31.0%; Figure 2B) is 40.2% of that seen in the non-CF culture (50.2 ± 4.7 μA/cm^2; Figure 2F). Second, this activity is 152% of that resulting from exposure of non-edited ΔF508/ΔF508 cells to the clinically approved CFTR modulators VX-809 and VX-770 (13.3 ± 0.9 μA/cm^2; Figure 2F). This particular combination of modulators has been shown to be of therapeutic benefit in ΔF508/ΔF508 CF patients[31] and thus provides a metric against which the CFTR activity in the edited ΔF508/ΔF508 cells can be compared. Thus, by both measures (% of non-CF, % of VX-809/VX-770 treated ΔF508/ΔF508), CFTR function resulting from this efficiency of ΔF508 correction is meaningful (see Discussion).

Similar analysis of ALI cultures derived from the 200-mer ssDNA donor-corrected airway basal cells (mean correction frequency of 10.6%; Figure 2B; Table S1) also demonstrated restored expression of mature CFTR protein (Figure S4), albeit at lower levels. For ssDNA donor edited cells, the level of CFTR current was 13.2% of the non-CF control (Tables S2A and S2B). However, rescue in this case did not reach the level of the VX-809/VX-770 treated ΔF508/ΔF508 control (21.3% of the non-CF control; Tables S2A and S2B). For sequence-specific ΔF508 correction, we observed an approximately linear correlation (R^2 = 0.92) between the frequency of correction and level of restored CFTR current (Figure 2G). Taken together, these data, comparing the ssDNA and AAV-6 donors, support the importance of achieving significant levels of editing.

tubulin (ACT) for ciliated cells. Representative 40× images in transverse section staining. Scale bar, 50 μm (panels). (D) Western blotting of CFTR. Sequence-specific ΔF508 correction restores expression of mature, fully glycosylated CFTR protein (band C). Calnexin, loading control. (E) Representative trace of short circuit current (Isc) from 4 samples tested: DMSO-treated, VX-809/VX-770 pre-treated and Z+D-treated CF (ΔF508/ΔF508), and non-CF evaluated by Ussing chamber analysis. (F) Summary of CFTR chloride current stimulated by forskolin and inhibited by CFTR inhibitor 172 (CFTR inh-172). Difference of Isc (ΔIsc) (μA/cm^2) before and after treatments are calculated from traces represented by (E). Values of ΔIsc from samples listed in Table S2 are summarized and shown (mean ± SD, n = 3 experiments). (G) Restored CFTR activity as function of gene-editing frequency. The blue symbols reflect results from individual ΔF508/ΔF508 cell experiments with sequence-specific correction of ΔF508 utilizing either ssDNA or AAV-6 donor. CFTR activity (forskolin-induced) for each experiment is expressed as % of non-CF (e.g., see Table S2A). Frequency of genome modification for each experiment is from Table S1. Shown in open and filled blue circles are results of ΔF508 correction for ΔF508/ΔF508 cells with ssDNA and AAV-6 donors, respectively; the black filled circle is from ΔF508/ΔF508 cells. Linear regression for ΔF508 sequence-specific correction experiments resulted in an R^2 = 0.92.

Efficient TI of *SA-CFTR*$_{9-27}$*-pA* into *CFTR* Intron 8 of ΔF508/ΔF508 Airway Basal Cells

We selected CFTR intron 8 to demonstrate proof of principle for the homologous recombination-mediated TI approach. ZFNs targeting *CFTR* intron 8 were designed and verified in K562 cells (data not shown). In order to facilitate simultaneous quantification of both the TI and indel frequencies in the same population of edited cells, an intron 8 specific primer, followed by a random sequence and an EcoRI site (to permit a rapid assessment of TI), was incorporated into the donor immediately downstream of the *SA-CFTR*$_{9-27}$*-pA* cassette (Figure 3A); PCR amplification would yield a PCR product of identical size as that from unmodified cells and NGS would permit an accurate determination of TI and indel rates. We note the downstream primer was positioned outside of donor sequences to only amplify from transgene sequences integrated at the targeted site (Figure 3A). Electroporation-mediated delivery of intron 8 ZFN mRNA to ΔF508/ΔF508 airway basal cells was followed almost immediately by AAV-6 transduction of *SA-CFTR*$_{9-27}$*-pA*. Initial evidence for sequence-specific TI of *SA-CFTR*$_{9-27}$*-pA* into intron 8 came from upstream inside-outside PCR amplification (Figure S5A) and from EcoRI digestion of downstream PCR amplicons (Figure S5B). These results were quantified by NGS, with TI rates of 56.5% ± 7.4% observed 4 days post editing (Figure 3B; Table S3A). Efficient intron 8 TI was confirmed by Southern blotting of genomic DNA isolated from the edited ΔF508/ΔF508 cells (Figure 3C).

TI of *SA-CFTR*$_{9-27}$*-pA* into *CFTR* Intron 8 of ΔF508/ΔF508 Airway Basal Cells Restores Mature CFTR Protein Expression and Function

Edited cells were plated in ALI cultures to develop well differentiated epithelium as described previously. In the one experiment for which we performed the analysis, we observed roughly comparable frequencies of intron 8 TI in basal cells prior to plating in the ALI cultures (50.1%) versus frequency of correction in mature, well differentiated airway epithelium in ALI cultures (43.9%) (Table S3B). The TI editing and minimal expansion required for early passage airway basal cell cultures also did not adversely affect the ability to establish well-differentiated airway epithelium comprising basal, secretory, and ciliated cells (Figure 3D). Successful TI-mediated correction of bulk cultures was confirmed by detection of *CFTR* transgene mRNA (Figure 3E) and by restoration of CFTR band C protein (Figure 3F). Using chamber assays from two independent experiments demonstrated restoration of forskolin-activated CFTR currents in intron 8 TI cultures (Figure 3G; sample trace in Figure S5C). CFTR current levels in edited cells from two independent experiments were 34.4% to 42.7% of the level seen in non-CF cultures (Figure 3G). Furthermore, the mean level of restored CFTR channel activity was 157% of the level seen for ΔF508/ΔF508 cultures exposed to VX-809/VX-770 (Figure 3G). Thus, with our current TI efficiency, we are in a therapeutically relevant range for a mixed population of corrected and uncorrected ΔF508/ΔF508 cells.

We also evaluated, in a limited number of experiments, the TI strategy for intron 7 by delivery of intron 7 specific ZFNs followed shortly thereafter by AAV-6 delivery of a donor construct now including *CFTR* exons 8 to 27 (*SA-CFTR*$_{8-27}$*-pA*). Evidence for intron 7 TI, first suggested via EcoRI digestion (Figure S6A), was confirmed by NGS (Figure S6B). Successful targeting was confirmed by expression of the transgenic mRNA (Figure S6C), restored CFTR band C protein (Figure S6D), and restored CFTR current (Figure S6E; sample trace in Figure S5C). This demonstrates that potential effectiveness of the TI approach is not limited to intron 8.

The level of TI-8 or TI-7 restored CFTR function in ΔF508/ΔF508 cells, as a function of editing efficiency, is shown in Figure 3H. These results confirm significant CFTR functional restoration with the TI approach. Given the limited number of experimental data points for either the sequence-specific correction or TI approaches, it is premature to draw any firm conclusions, However, the tendency of the TI data points to perhaps lie slightly below the sequence-specific trendline suggests that further improvements may be possible (see Discussion).

CFTR Intron 8 TI Preserves the Open Chromatin Structure of the ΔF508/ΔF508 *CFTR* Locus

Our rationale for directly targeting integration of the partial *CFTR* cDNA at the endogenous *CFTR* locus was to exploit the native *CFTR* promoter and chromatin architecture, with the goal of achieving physiologically relevant levels of restored CFTR protein and function. The presence in ALI cultures of transgene-derived *CFTR* mRNA (Figure 3E), protein (Figure 3F), and function (Figure 3G) from bulk TI-8 edited cells provides support for this targeting strategy. We further wished to confirm that neither the integrated *SA-CFTR*$_{9-27}$*-pA* transgene nor indels at the target site significantly disrupted the sites of open chromatin normally present in the native *CFTR* locus. To this end, we mapped, via Omni-ATAC-seq, the sites of open chromatin in ALI cultures established from TI-8 edited ΔF508/ΔF508 cells (Exp. 2; Table S3B; Figure 3G). At this time point, 43.9% and 47.3% of the *CFTR* alleles exhibited TI and indels, respectively (Table S3B). ALI cultures derived from unmanipulated ΔF508/ΔF508 cells or non-CF cells were used as controls. Significantly, Omni-ATAC-seq analysis of intron 8 targeted ALI cultures revealed minimal impact on the positions of open chromatin within the native *CFTR* locus (Figure 4). Unaffected sites of open chromatin included the *CFTR* topological domain boundaries at −80.1 kb and +48.9 kb, as well as the *CFTR* promoter and the previously identified −44 kb and −35 kb *cis*-regulatory elements (CREs) shown to play a critical role in directing *CFTR* expression in airway cells (Figure 4). Of note, other dominant peaks of open chromatin observed across the locus in HBE-ALI cells (all of which correspond to known CREs[32]) are also unaffected by the insertion. Upon closer examination, we did observe a new site of accessible chromatin near the start of the integrated *SA-CFTR*$_{9-27}$*-pA* transgene (Figure 4, lower panel). The significance of this particular finding is unclear. In summary, we find that intron 8 TI of the transgene has minimal impact on the open chromatin profile within the native *CFTR* locus.

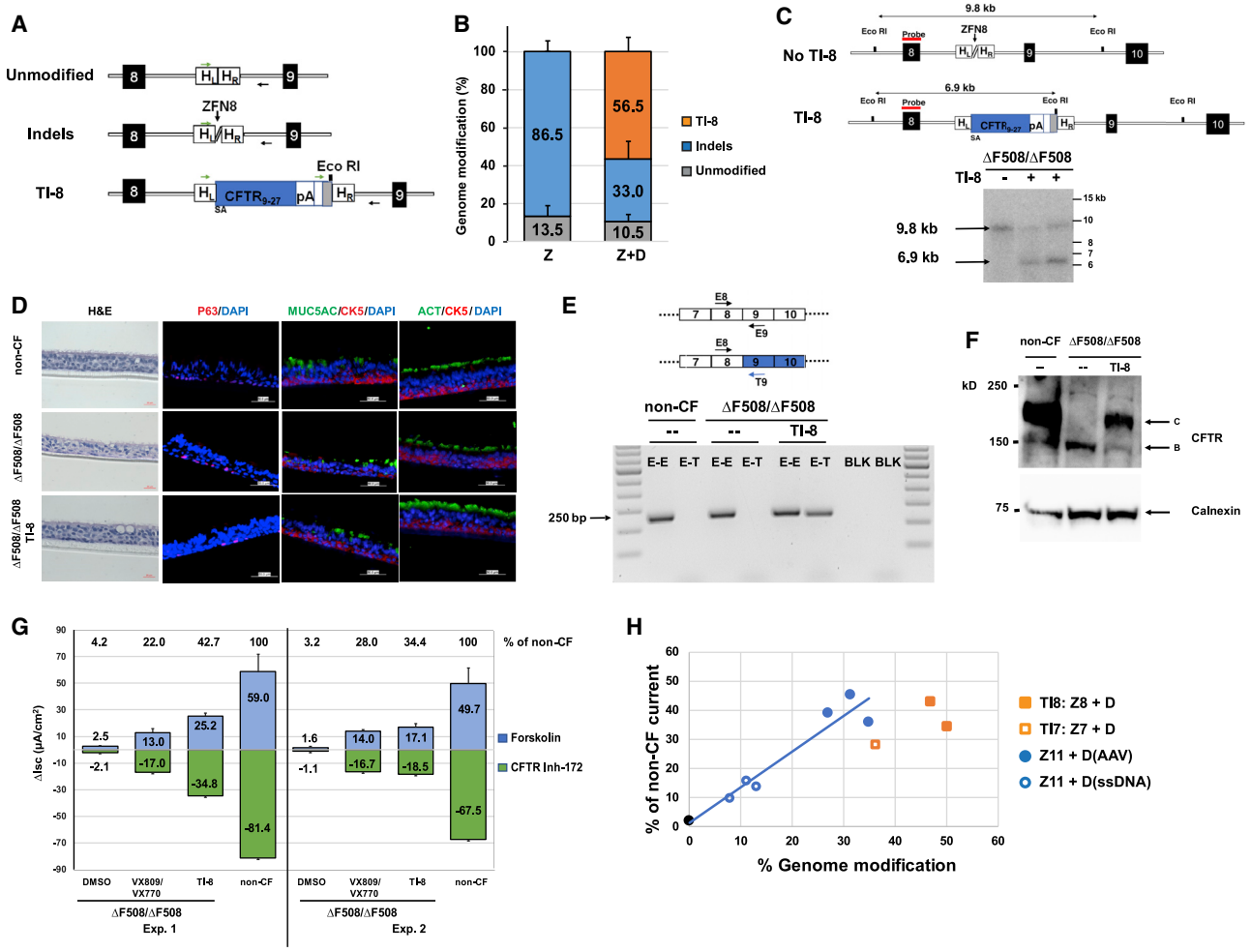

Figure 3. Efficient *SA-CFTR*$_{9-27}$*-pA* TI into *CFTR* Intron 8 of ΔF508/ΔF508 Airway Basal Cells

(A) Schematic of site-specific targeted editing of *CFTR* intron 8. Unmodified and indel diagrams highlight *CFTR* genomic sequences between exons 8 and 9 (black boxes; not to scale). TI-8 diagram shows intron 8 TI of human codon optimized *CFTR*$_{9-27}$ cDNA preceded by a splice acceptor, followed by bovine growth hormone (bGH) pA sequence, and flanked by 313 bp homology left (H_L) and 351 bp homology right (H_R) intron 8 sequences. Arrows indicate oligos amplifying unmodified, indel, or TI-8 events and used to quantify frequency of each by NGS. (B) The percentage of genome modification (mean ± SD) determined by NGS (Table S3A) from five independent TI-8 experiments (utilizing the AAV-6 donor at either 2×10^6 or 6×10^6 viral genomes [vg]/cell). There was no enhancement of TI efficiency as one increased the amount of donor. Efficiency was measured 4 days after the delivery of ZFNs targeting intron 8 (ZFN8) followed immediately by AAV-6 *CFTR*$_{9-27}$ cDNA donor. Z, ZFN8 alone; Z+D, ZFN8 and AAV-6 donor. (C) Southern blot analysis of TI-8. The schematic shows the expected genomic organization of non-targeted (no TI-8) and targeted (TI-8) alleles with the expected sizes resulting from EcoRI digestion. The non-targeted allele yields a 9.8 kb band while the TI-8 allele yields a 6.9 kb band due to the new EcoRI site in the *CFTR*$_{9-27}$ cDNA donor construct. (D) H&E staining and immunostaining of well-differentiated airway epithelium in ALI culture. Representative images of cross sections from ΔF508/ΔF508 or TI-8 ΔF508/ΔF508. Immunostaining shows major epithelial cell types: basal cell (CK5 and P63), secretory cells (MUC5AC), and ciliated cells (ACT). 40× images, scale bar, 50 μm. (E) Detection of transgene *CFTR*$_{9-27}$ mRNA. Schematic of endogenous and transgene *CFTR* mRNA is shown here. Primer T9 recognizes codon-optimized transgene exon 9 sequence only (blue) while Primer E9 recognizes endogenous exon 9. A 250 bp E8-T9 RT-PCR amplicon, evidence of the chimeric endogenous-transgene *CFTR* mRNA, was present only in the TI-8 ΔF508/ΔF508 sample. (F) Restoration of fully glycosylated CFTR protein via TI-8. Western blots of protein lysates harvested at 4 weeks of ALI culture. Band C, representing the mature, fully glycosylated form of CFTR, is present in non-CF, absent in ΔF508/ΔF508 cells, and restored in TI-8 ΔF508/ΔF508. Calnexin, loading control. (G) CFTR functional assay in ALI cultures at 4 weeks. TI-8 ΔF508/ΔF508 cells show the restoration of CFTR function measured as Δ Isc (μA/cm^2) ± SD and compared with ΔF508/ΔF508 treated with VX-809/VX-770. (H) Restored CFTR activity as function of gene-editing frequency. The blue and black symbols and blue linear regression line are from individual ΔF508/ΔF508 cell experiments with sequence-specific correction of ΔF508 (from Figure 2G). Shown in filled square and open square orange symbols are the results of ΔF508/ΔF508 cell TI-8 and ΔF508/ΔF508 cell TI-7 experiments, respectively.

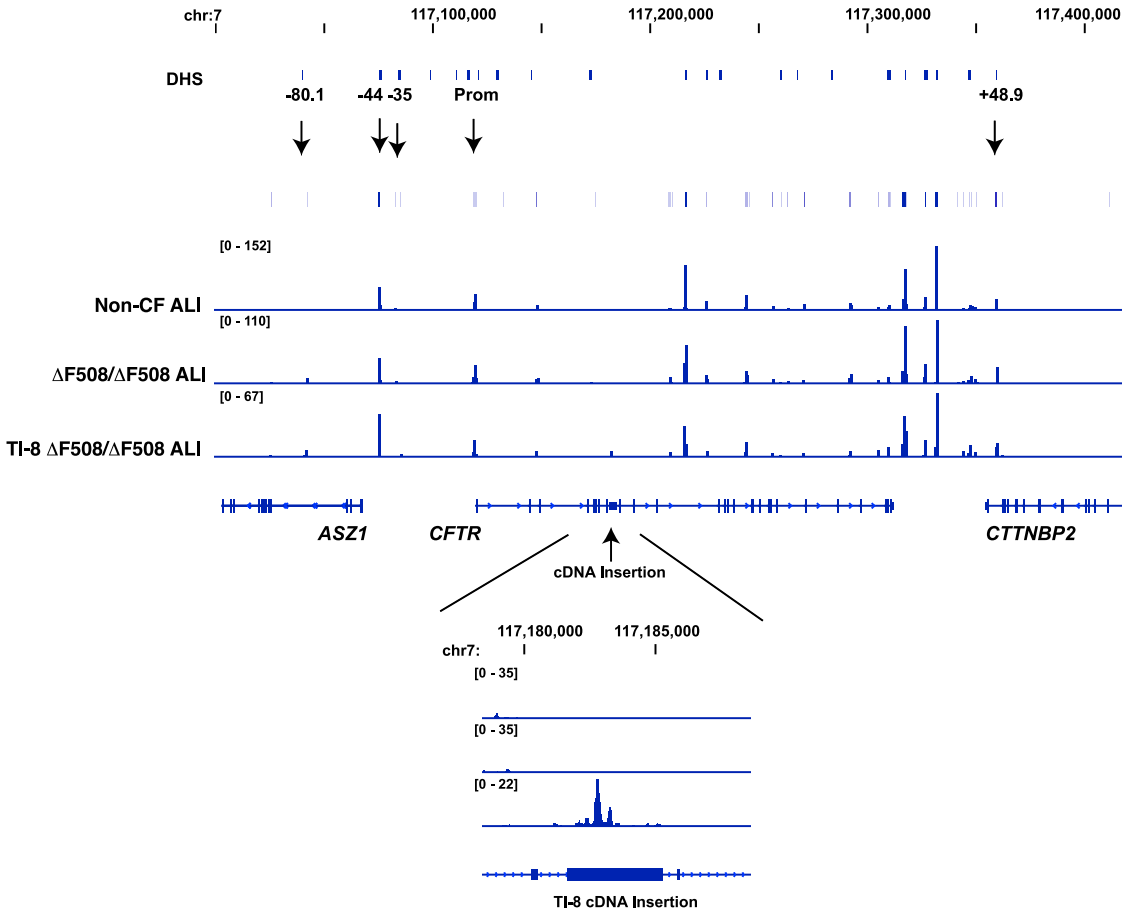

Figure 4. Targeted Integration of a Partial cDNA at *CFTR* Intron 8 Does Not Disrupt the Open Chromatin Profile of the ΔF508/ΔF508 *CFTR* Locus
Integrative Genomics Viewer (IGV) browser graphics of *CFTR* TAD regions showing Omni-ATAC profiles of non-CF, ΔF508/ΔF508, and TI-8 ΔF508/ΔF508 ALI cells. The number of sequencing reads is shown in Table S7. Key *cis*-regulatory elements are marked above the ATAC profiles by arrows. DHS denotes all DNase I-hypersensitive sites across the locus. Below is a magnified panel of the intron 8 region showing appearance of a peak of open chromatin at the TI-8 cDNA insertion site.

Efficient TI Restores Mature CFTR Protein Expression and Function in Airway Basal Cells Carrying *CFTR* Premature Termination Codon Mutations

TI strategies as described here are highly relevant to *CFTR* mutations resulting in little-or-no CFTR protein (for example, due to premature termination codons [PTCs] or splicing defects); i.e., variants not otherwise responsive to CFTR modulators. Evidence for sequence-specific TI of *SA-CFTR*$_{9\text{-}27}$*-pA* into intron 8 of ΔF508/R553X or G542X/R785X airway basal cells was obtained from 5′ inside-outside PCR amplification (Figure S7A). Amplification using 3′ PCR followed by EcoRI digestion was consistent with efficient TI (Figure S7B). NGS confirmed highly efficient TI in both the ΔF508/R553X (50.0% ± 6.0%) and G542X/R785X (61.8% ± 6.0%) airway basal cells (Tables S3C and S3D; Figure 5A), and efficient intron 8 TI was confirmed by Southern blot analysis (Figure 5B). Successful TI-mediated correction in the edited cultures was further established by restoration of CFTR band C protein (Figure 5C). Ussing chamber assays demonstrated restoration of forskolin-activated CFTR current in intron 8 TI ALI cultures at levels 55.8% of non-CF cultures for ΔF508/R553X and 33.8% of non-CF for G542X/R785X cultures (Figure 5D; sample traces in Figures S7C and S7D). These results demonstrate that targeted correction of PTC containing airway cells results in significant restoration of CFTR channel activity, either when the PTC occurs in combination with ΔF508 or with a second PTC.

DISCUSSION

In this study we have demonstrated highly efficient editing of the mutant *CFTR* locus in primary CF airway basal cells. High efficiency was achieved utilizing either a mutation-specific approach, demonstrated for correction of ΔF508, or a mutation-agnostic approach, requiring only that the *CFTR* mutation lies downstream of the targeted integration. Our objective was to achieve an efficiency of gene editing such that neither selection (e.g., via drug selection or sorting) nor single-cell derived cloning would be required to obtain a pool of cells corrected at a sufficiently high level to be directly transplantable. We are not aware of prior reports demonstrating efficient TI in CF

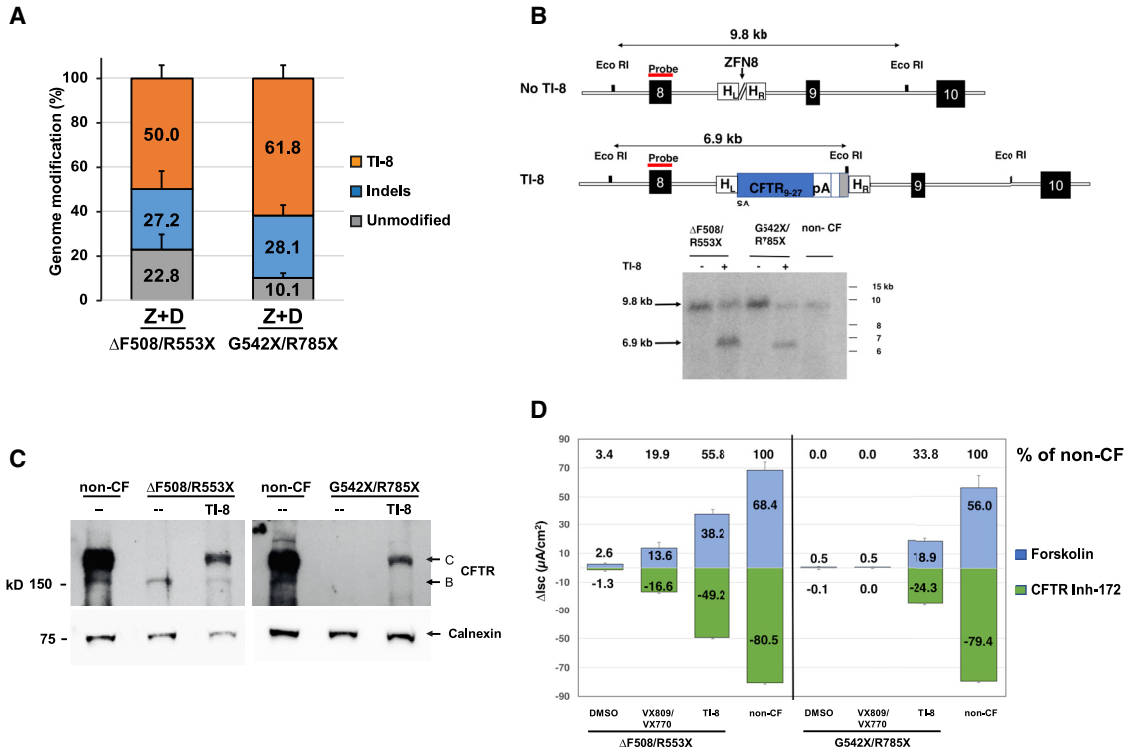

Figure 5. Efficient TI-8 Correction in CF Airway Basal Cells Carrying *CFTR* PTC Mutations

(A) Frequency of genome modification determined by NGS in CF basal cells carrying ΔF508/R553X (mean ± SD, n = 3 experiments) or G542X/R785X (mean ± SD, n = 4 experiments) variants (from Tables S3C and S3D). Highly efficient TI-8 was confirmed in CF basal cells treated with ZFN8 and AAV-6 $CFTR_{9\text{-}27}$ cDNA donor (Z+D) 4 days after genome editing. (B) Southern blot analysis of TI-8. A 6.9 kb fragment confirmed the expected TI-8 genomic organization in CF basal cells of either genotype. (C) Restoration of fully glycosylated CFTR protein via TI-8. Western blot of protein lysates harvested at 4 weeks of ALI culture shows the presence of band C in TI-8 and the absence in non-targeted cells. Calnexin, loading control. (D) CFTR functional assay in ALI cultures. Shown are short-circuit current measurements for bulk TI-8 ΔF508/R553X and TI-8 G542X/R785X cells. Restored CFTR currents are shown as ΔIsc (μA/cm^2) ± SD and are in excess of the VX-809/VX-770 treated cells. No VX-809/VX-770 response is expected for G542X/R785X.

primary airway basal stem cells; these levels of correction resulted in restored CFTR function for the basal cell-derived airway epithelium. Future studies will be required to determine how to prepare the CF airways for receipt and integration of the edited airway basal cells and how best to maximize the frequency of corrected cells in the resulting engrafted airway tissue.[33–35]

For ΔF508-specific correction utilizing AAV-6 donor delivery, we achieved correction to wild-type in approximately 30% of *CFTR* alleles. These editing results are generally similar to those recently reported for correction of ΔF508 in nasal and bronchial primary epithelial cells mediated by CRISPR/Cas9 together with AAV-6.[11] This 30% correction frequency corresponds to between 30% (if both ΔF508 alleles per cell are restored) and 60% (if only one ΔF508 allele is corrected per cell) of target cells demonstrating correction. In principle, molecular characterization of individual basal cells or single-cell-derived basal cell clones could provide a more accurate quantitative assessment of correction (or indels) on a per cell basis;[36] this will be addressed in future studies. Importantly, neither the manipulations required for editing (i.e., electroporation, AAV-6 transduction) nor the editing itself (i.e., correction, indels) altered the development or cellular composition of the derived pseudostratified epithelium. Studies of various *CFTR* mutations suggest that even very modest levels of *CFTR* gene correction may provide therapeutic benefit. For example, as little as 4.7% of the normal level of wild-type *CFTR* mRNA is sufficient to result in a milder form of *CF*.[37] In another study, 8% of wild-type *CFTR* transcripts was suggested to be sufficient for normal lung function.[38] According to this measure, even our modest 10.6% ± 2.6% ΔF508 correction efficiency with the ssDNA oligo donor, resulting in 13.2% ± 3.2% of wild-type current levels, might offer partial therapeutic benefit. The restoration of CFTR activity to levels 40.2% ± 4.7% of non-CF, resulting from AAV-6 delivery of the 2 kb donor approximates a therapeutically beneficial range, and exceeds the CFTR activity resulting from VX-809/VX-770 treatment (26.7% ± 3.6% of non-CF). Whereas the restoration of CFTR activity in edited cultures is presumably due only to the fraction of cells with correction, it is possible that modulators act more generally. Administration of the VX-809/VX-770 drug combination to homozygous ΔF508 patients resulted in improvements in

FEV_1, reduced rate of pulmonary exacerbations, reduced events leading to hospitalization, and reduced use of intravenous antibiotics.[31]

For sequence-specific ΔF508 correction, we observed an approximately linear correlation (R^2 = 0.92) between the frequency of ΔF508 correction and level of restored CFTR current (Figure 2G). In mixing experiments of primary human airway cells, 10%:90%, 20%:80%, and 60%:40% mixtures of non-CF:ΔF508/ΔF508 cells yielded CFTR chloride current at levels ∼35%, 70%, and 100% that of non-CF cells;[27] a linear relationship between CFTR current and % non-CF cells was maintained up to approximately 20% non-CF cell percentages.[27] On first examination, our levels of CFTR activity, as a function of gene-corrected cells, might appear to be somewhat lower than would be predicted by the mixing experiments. However, it is difficult to make direct comparisons of this type since it is currently unknown precisely what percentage of our cells were corrected at both *CFTR* alleles (corresponding to the non-CF cells utilized in the mixing experiment described above) versus at only a single *CFTR* allele per cell (corresponding to a carrier state). Although it might be assumed that carrier state cells would have CFTR activity similar to that of non-CF cells, it has been suggested that presence of the ΔF508 protein can adversely affect the processing and chloride channel function of the wild-type CFTR protein.[39]

While the mutation-specific editing approach achieved efficient correction and restored CFTR activity, there are at least two potential drawbacks to this strategy. First is the potential requirement for a new set of editing reagents (e.g., sequence specific nuclease and donor) for each mutation or small region spanning several mutations. Although this may be warranted for a common mutation such as ΔF508, development of editing materials and performance of clinical trials for each individual variant would be difficult. Second, even in the presence of donor, a significant frequency of *CFTR* alleles with nuclease-induced indels was observed; based on other editing studies,[36] as well as our own experience (data not shown), introduction of indels at both alleles is expected to occur with some frequency. For *CFTR* mutations occurring within exon sequences (e.g., ΔF508), such residual indels would need to be examined to ensure there are not unintended consequences, for example the potential loss of response to current or future modulators.

As an alternative strategy capable of treating airway basal cells carrying various *CFTR* mutations, we demonstrated efficient TI of *CFTR* partial cDNA sequences into *CFTR* introns 7 and 8. We first showed successful intron 8 TI in ΔF508/ΔF508 cells at efficiencies 56.5% ± 7.4% as measured 4 days after editing. Again, the manipulations required for highly efficient editing (mean allele modification of 56.5% for TI and 33.0% for indels) did not adversely affect the ability to establish well-differentiated airway epithelium. Intron 8 TI of ΔF508/ΔF508 cells restored CFTR function to levels 34.4%–42.7% of non-*CF*.

By targeting integration of a *CFTR* partial cDNA to the endogenous *CFTR* locus, our intent was to retain, to the greatest extent possible, the regulated level and pattern of expression of the native gene. Importantly, Omni-ATAC-seq analysis of the ΔF508/ΔF508 TI-8 ALI culture revealed no apparent alteration in the pattern of open chromatin at previously identified regulatory sites within the *CFTR* locus. This result is encouraging with respect to maintaining physiologically regulated transgene expression. We also demonstrated successful TI and restoration of CFTR activity for TI-7. It is likely that the overall reduced TI-7 efficiency (with respect to TI-8) is due to the lower activity of the intron 7 ZFNs (with respect to the intron 8 ZFNs; Figures 3B and S6B)

Recently, there have been important advances in development of CF modulators (e.g., the recently available triple drug combination) potentially providing significant therapeutic benefit to the vast majority of CF patients.[40,41] Consequently, increased focus is now being devoted to developing novel therapeutic approaches for the 7% of CF patients who are unable to benefit from modulators, due to an insufficient amount of CFTR protein (e.g., due to PTCs or splicing mutations). We thus applied the TI methodology to restore CFTR function in CF airway basal cells carrying PTCs. Again, we demonstrated highly efficient TI-8 at frequencies 50.0% ± 6.0% and 61.8% ± 6.0% in ΔF508/R553X and G542X/R785X cells, respectively (Figures 5A and 5B). After differentiation in ALI culture, restoration of both CFTR protein (Figure 5C) and function (Figure 5D) were observed.

In this project we evaluated TI for both introns 7 and 8. There are several considerations relevant to determining which *CFTR* intron is optimal for TI. One consideration would be to maximize the number of CF patients (or *CFTR* mutations) that could, in principle, benefit from site-specific TI. We note that intron 8 TI, for example, would provide correction for 89.1% of the CF-causing *CFTR* alleles listed in the CFTR2 database: https://www.cftr2.org/ (March 2019 version). Notably, this includes ΔF508, several of the most common PTCs such as G542X, R785X, and W1282X, and common splicing mutations such as 3,849 + 10 kb C > T. A second consideration is the size of the requisite *CFTR* partial cDNA and whether this can be appropriately delivered with a chosen vector. Although intron 1 targeting would appear to be preferred (by providing correction for all downstream mutations), limitations on packaging size for AAVs (∼4.7 kb) potentially precludes incorporating *SA-CFTR$_{2\text{-}27}$-pA* together with homology arms of sufficient size for efficient homology directed repair. A third aspect comprises the need to achieve integration without disrupting activity of critical CREs and the chromatin architecture of the *CFTR*.

A further consideration in the selection of which intron to target involves the relative strength(s) of the transgene splice acceptor versus the native splice acceptor in the immediate downstream *CFTR* exon. If the targeted intron were immediately upstream of a strong splice acceptor sequence, then it is possible that a significant amount of splicing could jump across the corrective partial *CFTR* cDNA. We

previously noted that the level of CFTR activity, as a function of editing frequency for either TI-7 or TI-8 (Figure 3H), was perhaps suggestive of a reduction relative to that resulting from the same frequency of site-specific correction. To quantitatively assess what fraction of *CFTR* mRNA transcripts from targeted alleles were spliced from the endogenous exon 8 to the transgenic exon 9 (thus including transgenic corrective sequences) versus alternative splicing downstream to the endogenous exon 9 (including only endogenous mutant sequences), we examined several single-cell-derived clones exhibiting homozygous intron 8 TI (Figures S8A–S8C). Quantitative RT-PCR demonstrated that the majority (58.0%–89.9%; depending on the clone) of *CFTR* transcripts exhibited the desired splicing from the endogenous exon 8 into the corrective human codon optimized exon 9 sequences; however, 10.1%–42.0% of transcripts did, in fact, reflect splicing across the corrective exon sequences directly into endogenous mutant exon 9 sequences (Figure S8D). A failure to capture only corrective cDNA sequences in *CFTR* mRNA transcripts from successfully targeted alleles would potentially result in reduced levels of CFTR protein and activity as a function of editing frequency. This finding perhaps suggests room for improvement in the TI strategy (e.g., strengthening either the splice acceptor sequence or, alternatively the poly-adenylation sequence to maximize termination of transcription). In addition, it is possible that our use of non-native amino acid-encoding transgene sequences (i.e., human codon optimized) may influence the efficiency of generating the appropriately folded CFTR protein necessary for functional activity.[42]

For any gene-editing approach, it is important to assess the nature and incidence of off-target effects that could potentially affect therapeutic safety. We experimentally identified via unbiased genome-wide oligonucleotide capture, in K562 cells, potential off-target sites (Table S4) for the intron 8-specific ZFNs employed in the editing experiments reported in this study;[43] we then quantitatively assessed the incidence of off-target indels in ZFN-treated primary ΔF508/ΔF508 airway basal cells (Figure S9A). This validated the occurrence of indels at varying frequency at 10 of the previously identified off-target sites. Although all of these sites lie in intergenic or intronic sequences (Figure S9A), we chose to optimize the ZFN design, in order to reduce the frequency of such off-target indels, while still retaining recognition of the same intended target sequences.[44] The improved intron 8 ZFNs maintained efficient on-target cleavage while exhibiting a significantly reduced incidence of off-target indels (Figure S9A). Importantly, the optimized ZFNs facilitated intron 8 TI of ΔF508/ΔF508 airway basal cells (Figures S9B and S9C) at levels similar to the original ZFNs.

Although we utilized airway epithelial cells from explanted lungs in these experiments, recently developed methodologies are capable of significantly expanding (*ex vivo*) the number of airway basal cells present in accessible primary tissues of CF patients, e.g., bronchial brushings (Figure S1A).[28,45] These developments make possible the consideration of autologous, tissue-resident basal cells from CF patients, and their editing for therapeutic use. We have readily expanded basal cells obtained from airway brushings and do not anticipate any difficulty in obtaining greater than the 6×10^7 cells estimated to be required for engraftment in a human lung.[33,46] There is compelling clinical evidence that small airways are a critical site of early obstruction and disease.[47] We expect that our studies using basal cells from the large airways (bronchi) will be representative of basal cells from bronchioles—an assertion that will require formal testing in the future.

With the objective of generating *CFTR*-corrected patient-specific airway basal stem cells, we have performed gene editing directly in minimally expanded primary airway basal cells. It would, in principle, be possible to first correct for *CFTR* mutations in CF patient induced pluripotent stem cells (iPSCs) and then derive airway basal cells, provided that robust differentiation protocols can be developed. Whereas earlier work by our group and others utilized sequence-specific editing for correction of CF iPSCs,[6,9,16] the TI of partial *CFTR* cDNAs, as reported here, would represent a more generalizable approach.[5,7] Finally, we note that although the *CFTR* gene-editing strategies pursued in the present studies were exclusively evaluated on airway basal cells *ex vivo*, it is possible that these tools, appropriately vectored, may eventually be applied for *in vivo* correction.

MATERIALS AND METHODS

Complete methods can be found in the Supplemental Information online. All primary/secondary antibodies and oligos used in this report are listed in Tables S5 and S6, respectively. Human subject review was performed by University of Texas Health Science Center institutional review committee.

Culture of Airway Basal Cells

Passage 1 CF and non-CF airway epithelial cells in this study were obtained from the Tissue Procurement and Cell Culture core facility at the University of North Carolina (Chapel Hill, NC, USA). Lungs were obtained following informed consent under UNC Office of Human Research Ethics/Institutional Review Board Study #03-1396 and cells were isolated as previously described.[48] Basal cells were cultured with Pneumacult-Ex Plus medium (StemCell Technologies, Vancouver, BC, Canada) on plates pre-coated with 804G cell-conditioned medium (CM) and maintained at 37°C in humidified air with 5% CO_2. At 50%–70% confluence, cells were dissociated by trypsinization and either re-plated at a 1:10 ratio or directly utilized for gene editing.

Gene Editing

Gene editing of basal cells was performed by electroporation-mediated delivery of ZFN mRNA (2–3 μg per reaction) followed immediately by AAV-6 donor transduction. Electroporations in this study were performed with the BTX ECM 830 electroporation generator (Harvard Apparatus, Holliston, MA, USA). The ZFN mRNA-electroporated cells were immediately transduced with AAV-6 donor at a multiplicity of infection (MOI) of $2 - 6 \times 10^6$ viral genomes per cell (vg/cell) overnight. Alternatively, for single-strand oligo DNA donors (ssDNA), basal cells were co-electroporated with ZFN mRNA and ssDNA and directly plated. All donor DNA sequences are shown in the Supplemental Information (donor DNA sequences).

Assessment of Genome Modification

The efficiency of induction of on-target indels, sequence-specific correction, and targeted integration was assessed quantitatively through NGS deep sequencing on the Illumina platform. Examples of sequencing data are uploaded in supplemental data files (Data S1 and S2). Additionally, targeted integration was confirmed by Southern blot analysis.

In Vitro Differentiation of Basal Cells at Air Liquid Interface (ALI)

200,000 airway basal cells were seeded on a 6.5 mm Transwell with 0.4 μm pore polyester membrane inserts (Corning, Corning, NY, USA) pre-coated with 804G-CM and subject to air liquid interface culture with Pneumacult-ALI medium (StemCell Technologies) for up to 4 weeks. Fully differentiated airway epithelia were confirmed by hematoxylin and eosin (H&E) staining and immunofluorescence analysis.

Molecular and Functional Analysis

ALI-cultured cells were assayed for *CFTR* mRNA expression with RT-PCR, CFTR protein expression via western blotting, and the functional CFTR correction by Ussing chamber analysis as described previously with modification.[16]

Omni Assay for Transposase Accessible Chromatin and Deep Sequencing

Omni-ATAC-seq was performed on 50,000 cells as described previously with minor modifications.[49] Omni-ATAC-seq libraries were purified with Agencourt AMPure XP magnetic beads (Beckman Coulter, Brea, CA, USA) with a sample to bead ratio of 1:1.2, and eluted in Buffer EB (Hilden, Germany). Libraries were pooled and sequenced on a HiSeq4000 machine (Illumina, San Diego, CA, USA) with 100 bp paired end reads. Data were processed by the ENCODE-DCC/atac-seq-pipeline. A custom genome was constructed using the Reform package (ver. August 2019) (https://github.com/gencorefacility/reform) to insert the partial cDNA sequence into the hg19 genome build.

SUPPLEMENTAL INFORMATION

Supplemental Information can be found online at https://doi.org/10.1016/j.ymthe.2020.04.021.

AUTHOR CONTRIBUTION

Conceptualization: B.R.D., A.C., A.H.; Project Administration: B.R.D., A.C., E.J.S., A.H.; Supervision: S.S.; Funding Acquisition: B.R.D., A.C., E.J.S., A.H., S.H.R.; Methodology: S.S., A.M.C., N.M.; Investigation: S.S., A.M.C., V.A., N.M., C.B., A.R., J.L.K., S.Y., M.M., K.K.; ZFN Design: L.Z.; Resources: S.H.R.; Writing – Original Draft: B.R.D., A.C., S.S., A.M.C., A.H.; Writing – Review & Editing: B.R.D., A.C., S.S., A.M.C., C.B., A.H., S.H.R., J.L.K., E.J.S.

CONFLICTS OF INTEREST

A.C., M.M., K.K., and L.Z. are employees of Sangamo Therapeutics.

ACKNOWLEDGMENTS

We gratefully acknowledge funding agencies enabling this study: Cystic Fibrosis Foundation (CFF): SANGAM16X0 to A.C., DAVIS15XX0 and DAVIS17XX0 to B.R.D., RANDEL15XX0, RANDEL17XX0, and BOUCHE15RO to S.H.R., and HARRIS15/17XX0, HARRIS16G0, and HARRIS18P0 to A.H.; National Institutes of Health (NIH): R01 HL139876 to E.J.S. and B.R.D., DK065988 to S.H.R., and R01 HL094585 to AH; and UTHealth Pulmonary Center of Excellence to B.R.D. We also acknowledge histological sample preparation by Dr. Zhengmei Mao (UTHealth Microscopy Core Facility), Dr. Susan Reynolds for guidance and discussions, and Dr. Hongmei Mou for guidance on the dual SMAD inhibition expansion methodology and providing the 804G cell line.

REFERENCES

1. Hogan, B.L., Barkauskas, C.E., Chapman, H.A., Epstein, J.A., Jain, R., Hsia, C.C., Niklason, L., Calle, E., Le, A., Randell, S.H., et al. (2014). Repair and regeneration of the respiratory system: complexity, plasticity, and mechanisms of lung stem cell function. Cell Stem Cell *15*, 123–138.
2. Rock, J.R., Onaitis, M.W., Rawlins, E.L., Lu, Y., Clark, C.P., Xue, Y., Randell, S.H., and Hogan, B.L. (2009). Basal cells as stem cells of the mouse trachea and human airway epithelium. Proc. Natl. Acad. Sci. USA *106*, 12771–12775.
3. Rock, J.R., Randell, S.H., and Hogan, B.L. (2010). Airway basal stem cells: a perspective on their roles in epithelial homeostasis and remodeling. Dis. Model. Mech. *3*, 545–556.
4. Hong, K.U., Reynolds, S.D., Watkins, S., Fuchs, E., and Stripp, B.R. (2004). Basal cells are a multipotent progenitor capable of renewing the bronchial epithelium. Am. J. Pathol. *164*, 577–588.
5. Harrison, P.T., Hoppe, N., and Martin, U. (2018). Gene editing & stem cells. J. Cyst. Fibros. *17*, 10–16.
6. Firth, A.L., Menon, T., Parker, G.S., Qualls, S.J., Lewis, B.M., Ke, E., Dargitz, C.T., Wright, R., Khanna, A., Gage, F.H., and Verma, I.M. (2015). Functional gene correction for cystic fibrosis in lung epithelial cells generated from patient ipscs. Cell Rep. *12*, 1385–1390.
7. Bednarski, C., Tomczak, K., Vom Hövel, B., Weber, W.M., and Cathomen, T. (2016). Targeted integration of a super-exon into the cftr locus leads to functional correction of a cystic fibrosis cell line model. PLoS ONE *11*, e0161072.
8. Merkert, S., Bednarski, C., Göhring, G., Cathomen, T., and Martin, U. (2017). Generation of a gene-corrected isogenic control iPSC line from cystic fibrosis patient-specific iPSCs homozygous for p.Phe508del mutation mediated by TALENs and ssODN. Stem Cell Res. (Amst.) *23*, 95–97.
9. Suzuki, S., Sargent, R.G., Illek, B., Fischer, H., Esmaeili-Shandiz, A., Yezzi, M.J., Lee, A., Yang, Y., Kim, S., Renz, P., et al. (2016). Talens facilitate single-step seamless sdf correction of f508del cftr in airway epithelial submucosal gland cell-derived cf-ipscs. Mol. Ther. Nucleic Acids *5*, e273.
10. Maule, G., Casini, A., Montagna, C., Ramalho, A.S., De Boeck, K., Debyser, Z., Carlon, M.S., Petris, G., and Cereseto, A. (2019). Allele specific repair of splicing mutations in cystic fibrosis through AsCas12a genome editing. Nat. Commun. *10*, 3556.
11. Vaidyanathan, S., Salahudeen, A.A., Sellers, Z.M., Bravo, D.T., Choi, S.S., Batish, A., Le, W., Baik, R., de la, O.S., Kaushik, M.P., et al. (2020). High-efficiency, selection-free gene repair in airway stem cells from cystic fibrosis patients rescues cftr function in differentiated epithelia. Cell Stem Cell *26*, 161–171.
12. Jennings, S., Ng, H.P., and Wang, G. (2019). Establishment of a ΔF508-CF promyelocytic cell line for cystic fibrosis research and drug screening. J. Cyst. Fibros. *18*, 44–53.
13. Ruan, J., Hirai, H., Yang, D., Ma, L., Hou, X., Jiang, H., Wei, H., Rajagopalan, C., Mou, H., Wang, G., et al. (2019). Efficient gene editing at major cftr mutation loci. Mol. Ther. Nucleic Acids *16*, 73–81.
14. Ramalingam, S., London, V., Kandavelou, K., Cebotaru, L., Guggino, W., Civin, C., and Chandrasegaran, S. (2013). Generation and genetic engineering of human

induced pluripotent stem cells using designed zinc finger nucleases. Stem Cells Dev. *22*, 595–610.

15. Valley, H.C., Bukis, K.M., Bell, A., Cheng, Y., Wong, E., Jordan, N.J., Allaire, N.E., Sivachenko, A., Liang, F., Bihler, H., et al. (2019). Isogenic cell models of cystic fibrosis-causing variants in natively expressing pulmonary epithelial cells. J. Cyst. Fibros. *18*, 476–483.
16. Crane, A.M., Kramer, P., Bui, J.H., Chung, W.J., Li, X.S., Gonzalez-Garay, M.L., Hawkins, F., Liao, W., Mora, D., Choi, S., et al. (2015). Targeted correction and restored function of the CFTR gene in cystic fibrosis induced pluripotent stem cells. Stem Cell Reports *4*, 569–577.
17. Sinn, P.L., Hwang, B.Y., Li, N., Ortiz, J.L.S., Shirazi, E., Parekh, K.R., Cooney, A.L., Schaffer, D.V., and McCray, P.B., Jr. (2017). Novel GP64 envelope variants for improved delivery to human airway epithelial cells. Gene Ther. *24*, 674–679.
18. Cooney, A.L., Thornell, I.M., Singh, B.K., Shah, V.S., Stoltz, D.A., McCray, P.B., Jr., Zabner, J., and Sinn, P.L. (2019). Novel aav-mediated gene delivery system corrects cftr function in pigs. Am. J. Respir. Cell Mol. Biol. *61*, 747–754.
19. Cmielewski, P., Donnelley, M., and Parsons, D.W. (2014). Long-term therapeutic and reporter gene expression in lentiviral vector treated cystic fibrosis mice. J. Gene Med. *16*, 291–299.
20. Yan, Z., McCray, P.B., Jr., and Engelhardt, J.F. (2019). Advances in gene therapy for cystic fibrosis lung disease. Hum. Mol. Genet. *28* (R1), R88–R94.
21. Steines, B., Dickey, D.D., Bergen, J., Excoffon, K.J., Weinstein, J.R., Li, X., Yan, Z., Abou Alaiwa, M.H., Shah, V.S., Bouzek, D.C., et al. (2016). *CFTR* gene transfer with AAV improves early cystic fibrosis pig phenotypes. JCI Insight *1*, e88728.
22. Montoro, D.T., Haber, A.L., Biton, M., Vinarsky, V., Lin, B., Birket, S.E., Yuan, F., Chen, S., Leung, H.M., Villoria, J., et al. (2018). A revised airway epithelial hierarchy includes CFTR-expressing ionocytes. Nature *560*, 319–324.
23. Plasschaert, L.W., Žilionis, R., Choo-Wing, R., Savova, V., Knehr, J., Roma, G., Klein, A.M., and Jaffe, A.B. (2018). A single-cell atlas of the airway epithelium reveals the CFTR-rich pulmonary ionocyte. Nature *560*, 377–381.
24. Okuda, K., Kobayashi, Y., Dang, H., Nakano, S., Barbosa Cardenas, S.M., On, V.K., Kato, T., Chen, G., Gilmore, R.C., Chua, M., et al. (2019). Regional regulation of cftr and ionocyte expression in normal human airways. 2019 North American CF Conference, Nashville TN, Pediatric Pulmonology, *54*, Abstract 48.
25. Johnson, L.G., Olsen, J.C., Sarkadi, B., Moore, K.L., Swanstrom, R., and Boucher, R.C. (1992). Efficiency of gene transfer for restoration of normal airway epithelial function in cystic fibrosis. Nat. Genet. *2*, 21–25.
26. Goldman, M.J., Yang, Y., and Wilson, J.M. (1995). Gene therapy in a xenograft model of cystic fibrosis lung corrects chloride transport more effectively than the sodium defect. Nat. Genet. *9*, 126–131.
27. Farmen, S.L., Karp, P.H., Ng, P., Palmer, D.J., Koehler, D.R., Hu, J., Beaudet, A.L., Zabner, J., and Welsh, M.J. (2005). Gene transfer of CFTR to airway epithelia: low levels of expression are sufficient to correct Cl- transport and overexpression can generate basolateral CFTR. Am. J. Physiol. Lung Cell. Mol. Physiol. *289*, L1123–L1130.
28. Mou, H., Vinarsky, V., Tata, P.R., Brazauskas, K., Choi, S.H., Crooke, A.K., Zhang, B., Solomon, G.M., Turner, B., Bihler, H., et al. (2016). Dual smad signaling inhibition enables long-term expansion of diverse epithelial basal cells. Cell Stem Cell *19*, 217–231.
29. Limberis, M.P., Vandenberghe, L.H., Zhang, L., Pickles, R.J., and Wilson, J.M. (2009). Transduction efficiencies of novel AAV vectors in mouse airway epithelium in vivo and human ciliated airway epithelium in vitro. Mol. Ther. *17*, 294–301.
30. Yan, Z., Lei-Butters, D.C., Keiser, N.W., and Engelhardt, J.F. (2013). Distinct transduction difference between adeno-associated virus type 1 and type 6 vectors in human polarized airway epithelia. Gene Ther. *20*, 328–337.
31. Wainwright, C.E., Elborn, J.S., Ramsey, B.W., Marigowda, G., Huang, X., Cipolli, M., Colombo, C., Davies, J.C., De Boeck, K., Flume, P.A., et al.; TRAFFIC Study Group; TRANSPORT Study Group (2015). Lumacaftor-ivacaftor in patients with cystic fibrosis homozygous for phe508del cftr. N. Engl. J. Med. *373*, 220–231.
32. Swahn, H., and Harris, A. (2019). Cell-selective regulation of cftr gene expression: Relevance to gene editing therapeutics. Genes (Basel) *10*, E235.
33. Ghosh, M., Ahmad, S., White, C.W., and Reynolds, S.D. (2017). Transplantation of airway epithelial stem/progenitor cells: A future for cell-based therapy. Am. J. Respir. Cell Mol. Biol. *56*, 1–10.
34. Milman Krentsis, I., Rosen, C., Shezen, E., Aronovich, A., Nathanson, B., Bachar-Lustig, E., Berkman, N., Assayag, M., Shakhar, G., Feferman, T., et al. (2018). Lung injury repair by transplantation of adult lung cells following preconditioning of recipient mice. Stem Cells Transl. Med. *7*, 68–77.
35. Farrow, N., Cmielewski, P., Donnelley, M., Rout-Pitt, N., Moodley, Y., Bertoncello, I., and Parsons, D. (2018). Epithelial disruption: a new paradigm enabling human airway stem cell transplantation. Stem Cell Res. Ther. *9*, 153.
36. Park, S.H., Lee, C.M., Dever, D.P., Davis, T.H., Camarena, J., Srifa, W., Zhang, Y., Paikari, A., Chang, A.K., Porteus, M.H., et al. (2019). Highly efficient editing of the β-globin gene in patient-derived hematopoietic stem and progenitor cells to treat sickle cell disease. Nucleic Acids Res. *47*, 7955–7972.
37. Ramalho, A.S., Beck, S., Meyer, M., Penque, D., Cutting, G.R., and Amaral, M.D. (2002). Five percent of normal cystic fibrosis transmembrane conductance regulator mRNA ameliorates the severity of pulmonary disease in cystic fibrosis. Am. J. Respir. Cell Mol. Biol. *27*, 619–627.
38. Chu, C.S., Trapnell, B.C., Curristin, S.M., Cutting, G.R., and Crystal, R.G. (1992). Extensive posttranscriptional deletion of the coding sequences for part of nucleotide-binding fold 1 in respiratory epithelial mRNA transcripts of the cystic fibrosis transmembrane conductance regulator gene is not associated with the clinical manifestations of cystic fibrosis. J. Clin. Invest. *90*, 785–790.
39. Tucker, T.A., Fortenberry, J.A., Zsembery, A., Schwiebert, L.M., and Schwiebert, E.M. (2012). The ΔF508-CFTR mutation inhibits wild-type CFTR processing and function when co-expressed in human airway epithelia and in mouse nasal mucosa. BMC Physiol. *12*, 12.
40. Keating, D., Marigowda, G., Burr, L., Daines, C., Mall, M.A., McKone, E.F., Ramsey, B.W., Rowe, S.M., Sass, L.A., Tullis, E., et al.; VX16-445-001 Study Group (2018). Vx-445-tezacaftor-ivacaftor in patients with cystic fibrosis and one or two phe508del alleles. N. Engl. J. Med. *379*, 1612–1620.
41. Middleton, P.G., Mall, M.A., Dřevínek, P., Lands, L.C., McKone, E.F., Polineni, D., Ramsey, B.W., Taylor-Cousar, J.L., Tullis, E., Vermeulen, F., et al.; VX17-445-102 Study Group (2019). Elexacaftor-tezacaftor-ivacaftor for cystic fibrosis with a single phe508del allele. N. Engl. J. Med. *381*, 1809–1819.
42. Kim, S.J., Yoon, J.S., Shishido, H., Yang, Z., Rooney, L.A., Barral, J.M., and Skach, W.R. (2015). Protein folding. Translational tuning optimizes nascent protein folding in cells. Science *348*, 444–448.
43. Tsai, S.Q., Zheng, Z., Nguyen, N.T., Liebers, M., Topkar, V.V., Thapar, V., Wyvekens, N., Khayter, C., Iafrate, A.J., Le, L.P., et al. (2015). GUIDE-seq enables genome-wide profiling of off-target cleavage by CRISPR-Cas nucleases. Nat. Biotechnol. *33*, 187–197.
44. Miller, J.C., Patil, D.P., Xia, D.F., Paine, C.B., Fauser, F., Richards, H.W., Shivak, D.A., Bendaña, Y.R., Hinkley, S.J., Scarlott, N.A., et al. (2019). Enhancing gene editing specificity by attenuating DNA cleavage kinetics. Nat. Biotechnol. *37*, 945–952.
45. Butler, C.R., Hynds, R.E., Gowers, K.H., Lee, Ddo.H., Brown, J.M., Crowley, C., Teixeira, V.H., Smith, C.M., Urbani, L., Hamilton, N.J., et al. (2016). Rapid expansion of human epithelial stem cells suitable for airway tissue engineering. Am. J. Respir. Crit. Care Med. *194*, 156–168.
46. Hayes, D., Jr., Kopp, B.T., Hill, C.L., Lallier, S.W., Schwartz, C.M., Tadesse, M., Alsudayri, A., and Reynolds, S.D. (2019). Cell therapy for cystic fibrosis lung disease: Regenerative basal cell amplification. Stem Cells Transl. Med. *8*, 225–235.
47. Rosenow, T., Ramsey, K., Turkovic, L., Murray, C.P., Mok, L.C., Hall, G.L., Stick, S.M., and Arest, C.F.; AREST CF (2017). Air trapping in early cystic fibrosis lung disease-Does CT tell the full story? Pediatr. Pulmonol. *52*, 1150–1156.
48. Fulcher, M.L., and Randell, S.H. (2013). Human nasal and tracheo-bronchial respiratory epithelial cell culture. Methods Mol. Biol. *945*, 109–121.
49. Corces, M.R., Trevino, A.E., Hamilton, E.G., Greenside, P.G., Sinnott-Armstrong, N.A., Vesuna, S., Satpathy, A.T., Rubin, A.J., Montine, K.S., Wu, B., et al. (2017). An improved ATAC-seq protocol reduces background and enables interrogation of frozen tissues. Nat. Methods *14*, 959–962.

YMTHE, Volume *28*

Supplemental Information

Highly Efficient Gene Editing of Cystic Fibrosis Patient-Derived Airway Basal Cells Results in Functional CFTR Correction

Shingo Suzuki, Ana M. Crane, Varada Anirudhan, Cristina Barillà, Nadine Matthias, Scott H. Randell, Andras Rab, Eric J. Sorscher, Jenny L. Kerschner, Shiyi Yin, Ann Harris, Matthew Mendel, Kenneth Kim, Lei Zhang, Anthony Conway, and Brian R. Davis

Fig. S1

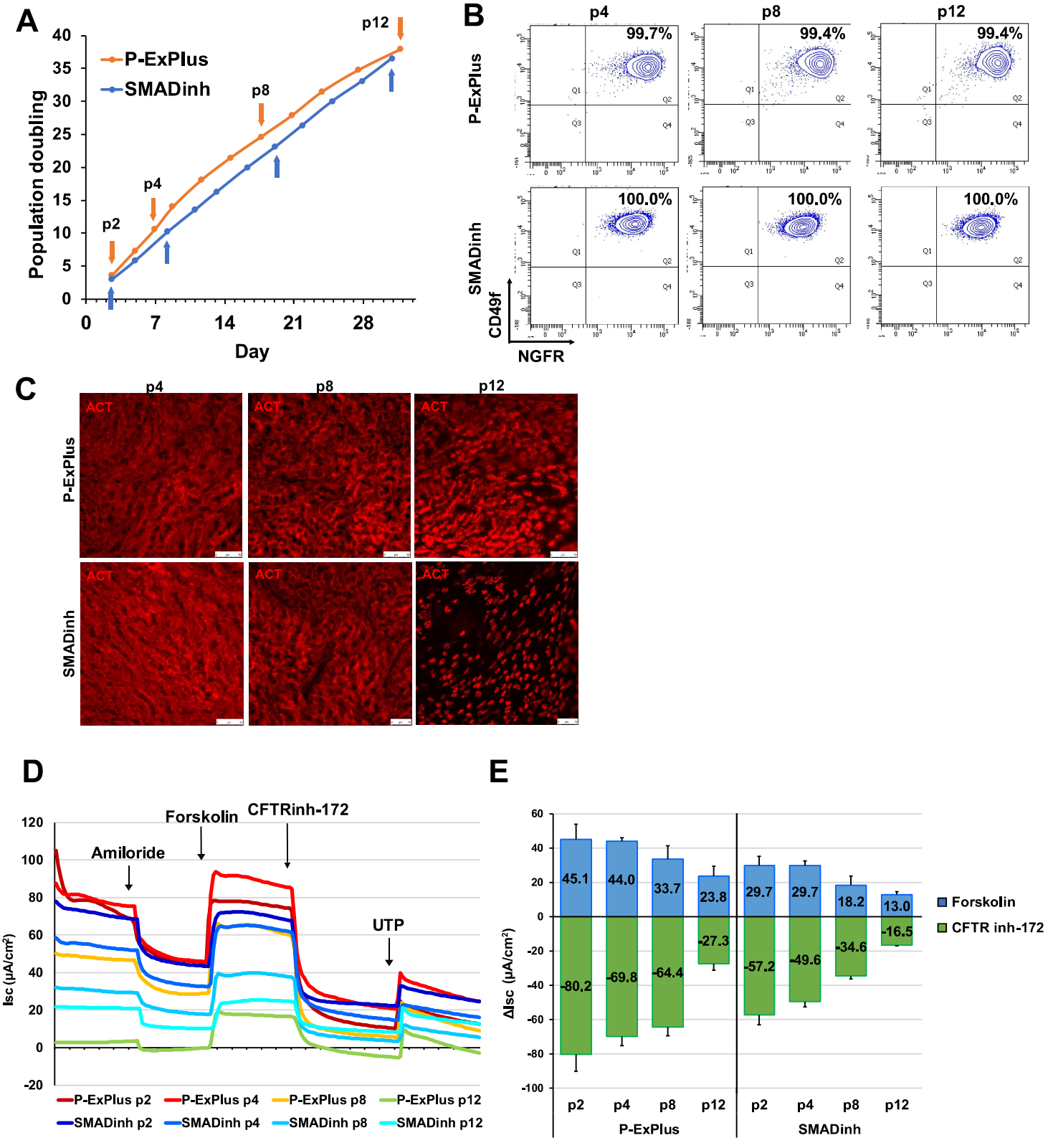
A
Population doubling
Day
P-ExPlus
SMADinh
p2
p4
p8
p12
B
p4
p8
p12
P-ExPlus
SMADinh
99.7%
99.4%
99.4%
100.0%
100.0%
100.0%
CD49f
NGFR
C
p4
p8
p12
P-ExPlus
SMADinh
ACT
D
Forskolin
CFTRinh-172
Amiloride
UTP
Isc (µA/cm²)
P-ExPlus p2
P-ExPlus p4
P-ExPlus p8
P-ExPlus p12
SMADinh p2
SMADinh p4
SMADinh p8
SMADinh p12
E
ΔIsc (µA/cm²)
45.1
44.0
33.7
23.8
29.7
29.7
18.2
13.0
-80.2
-69.8
-64.4
-27.3
-57.2
-49.6
-34.6
-16.5
p2
p4
p8
p12
P-ExPlus
SMADinh
Forskolin
CFTR inh-172

Fig. S2

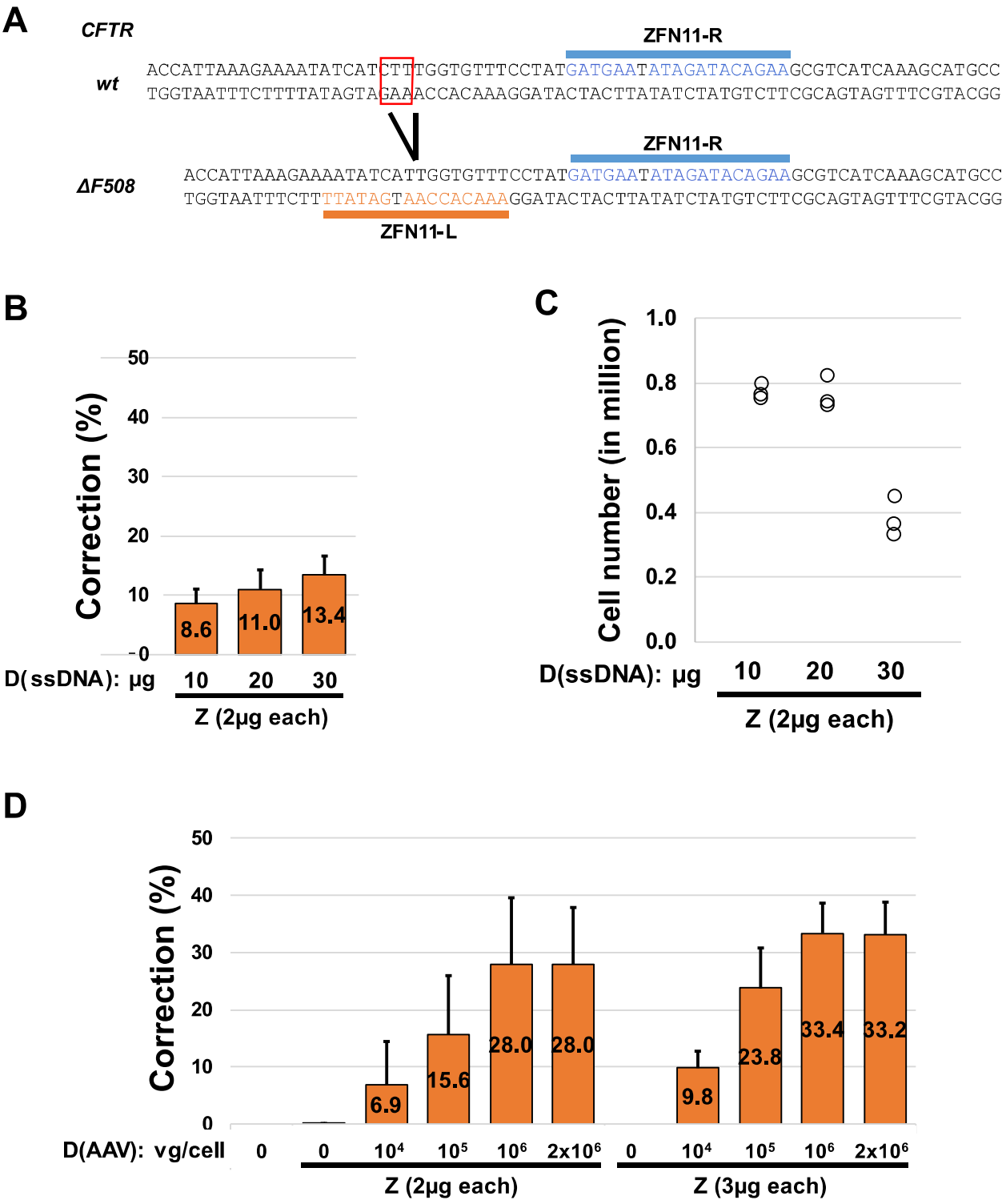
A
CFTR
ZFN11-R
wt
ACCATTAAAGAAAATATCATCTTTGGTGTTTCCTATGATGAATATAGATACAGAAGCGTCATCAAAGCATGCC
TGGTAATTTCTTTTATAGTAGAAACCACAAAGGATACTACTTATATCTATGTCTTCGCAGTAGTTTCGTACGG
ZFN11-R
ΔF508
ACCATTAAAGAAAATATCATTGGTGTTTCCTATGATGAATATAGATACAGAAGCGTCATCAAAGCATGCC
TGGTAATTTCTTTTATAGTAACCACAAAGGATACTACTTATATCTATGTCTTCGCAGTAGTTTCGTACGG
ZFN11-L
B
Correction (%)
50
40
30
20
10
0
8.6
11.0
13.4
D(ssDNA): μg
10
20
30
Z (2μg each)
C
Cell number (in million)
1.0
0.8
0.6
0.4
0.2
0.0
D(ssDNA): μg
10
20
30
Z (2μg each)
D
Correction (%)
50
40
30
20
10
0
6.9
15.6
28.0
28.0
9.8
23.8
33.4
33.2
D(AAV): vg/cell
0
0
10⁴
10⁵
10⁶
2x10⁶
0
10⁴
10⁵
10⁶
2x10⁶
Z (2μg each)
Z (3μg each)

Fig. S3

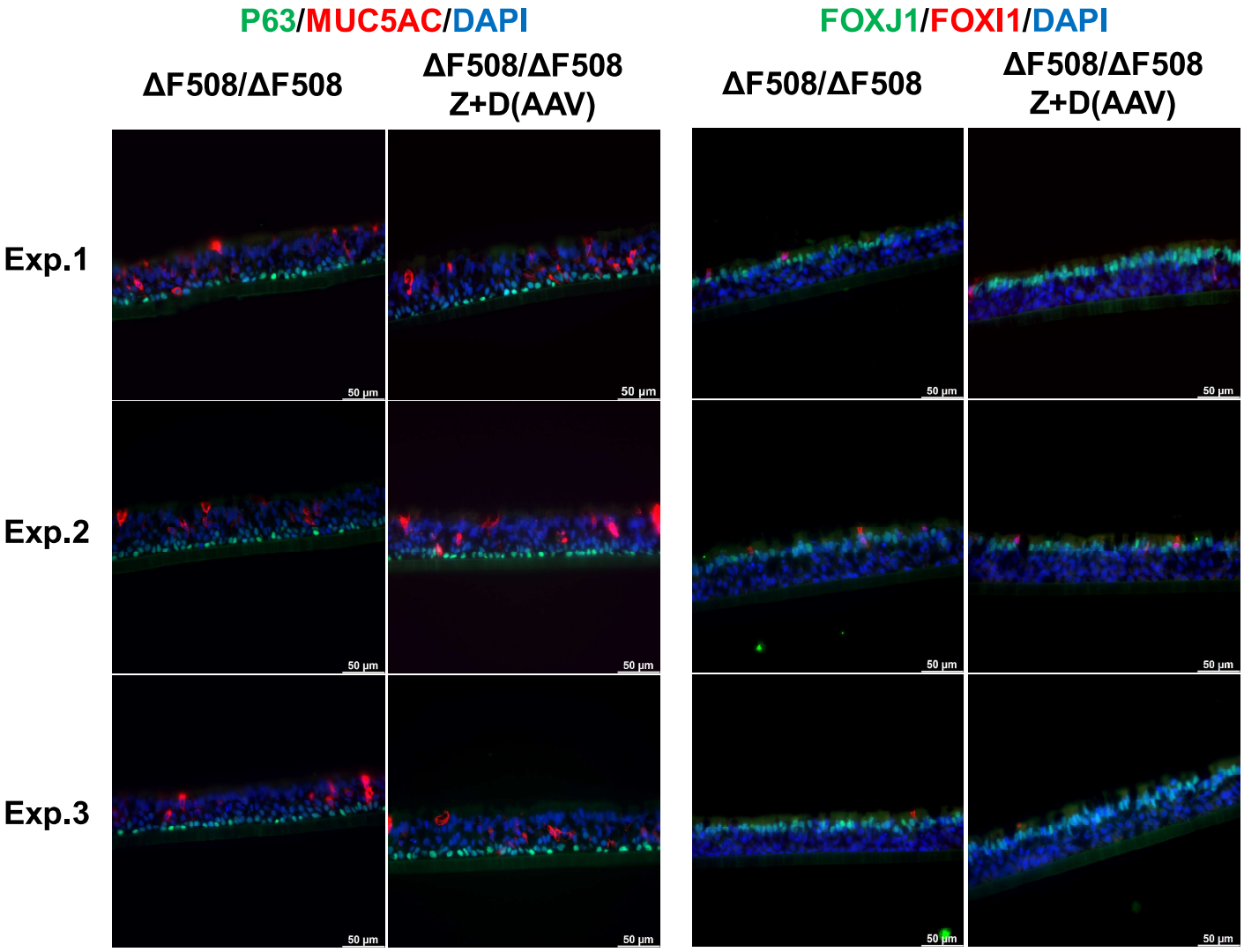
P63/MUC5AC/DAPI
FOXJ1/FOXI1/DAPI
ΔF508/ΔF508
ΔF508/ΔF508 Z+D(AAV)
ΔF508/ΔF508
ΔF508/ΔF508 Z+D(AAV)
Exp.1
Exp.2
Exp.3
50 μm

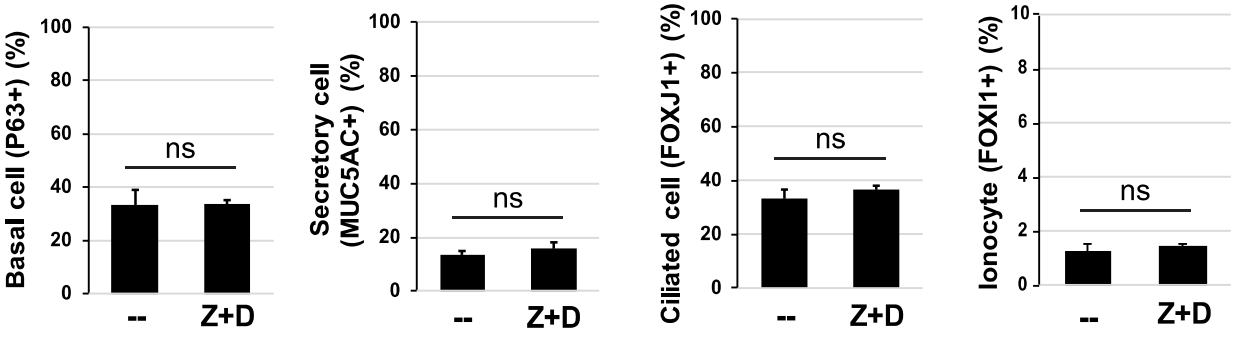
Basal cell (P63+) (%)
Secretory cell (MUC5AC+) (%)
Ciliated cell (FOXJ1+) (%)
Ionocyte (FOXI1+) (%)
ns
--
Z+D

Fig. S4

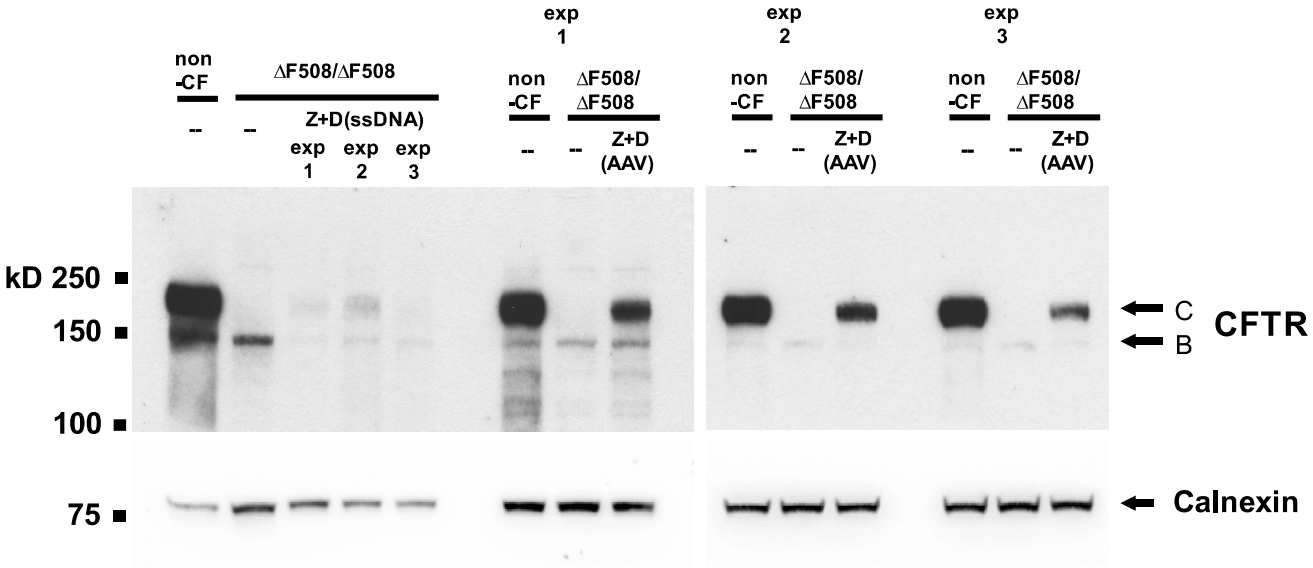
exp 1
exp 2
exp 3
non -CF
ΔF508/ΔF508
Z+D(ssDNA)
exp 1
exp 2
exp 3
non -CF
ΔF508/ ΔF508
Z+D (AAV)
non -CF
ΔF508/ ΔF508
Z+D (AAV)
non -CF
ΔF508/ ΔF508
Z+D (AAV)
kD 250
150
100
75
C
B
CFTR
Calnexin

Fig. S5

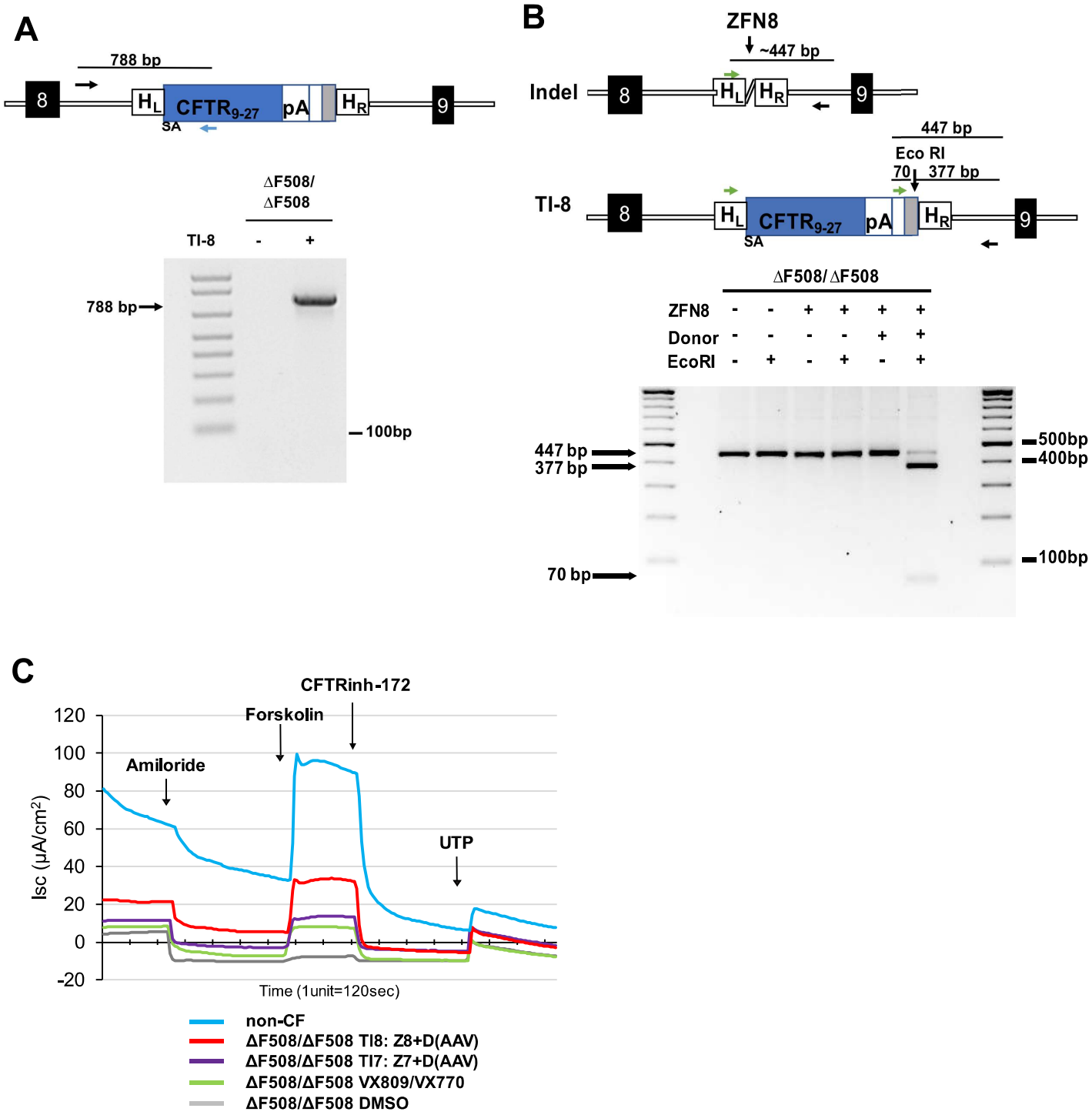
A
788 bp
8
HL
CFTR9-27
pA
HR
9
SA
ΔF508/
ΔF508
TI-8 - +
788 bp
100bp
B
ZFN8
~447 bp
Indel
8
HL
HR
9
447 bp
Eco RI
70 377 bp
TI-8
8
HL
CFTR9-27
pA
HR
9
SA
ΔF508/ΔF508
ZFN8 - - + + + +
Donor - - - - + +
EcoRI - + - + - +
447 bp
377 bp
70 bp
500bp
400bp
100bp
C
CFTRinh-172
Forskolin
Amiloride
UTP
Isc (μA/cm2)
120
100
80
60
40
20
0
-20
Time (1unit=120sec)
non-CF
ΔF508/ΔF508 TI8: Z8+D(AAV)
ΔF508/ΔF508 TI7: Z7+D(AAV)
ΔF508/ΔF508 VX809/VX770
ΔF508/ΔF508 DMSO

Fig. S6

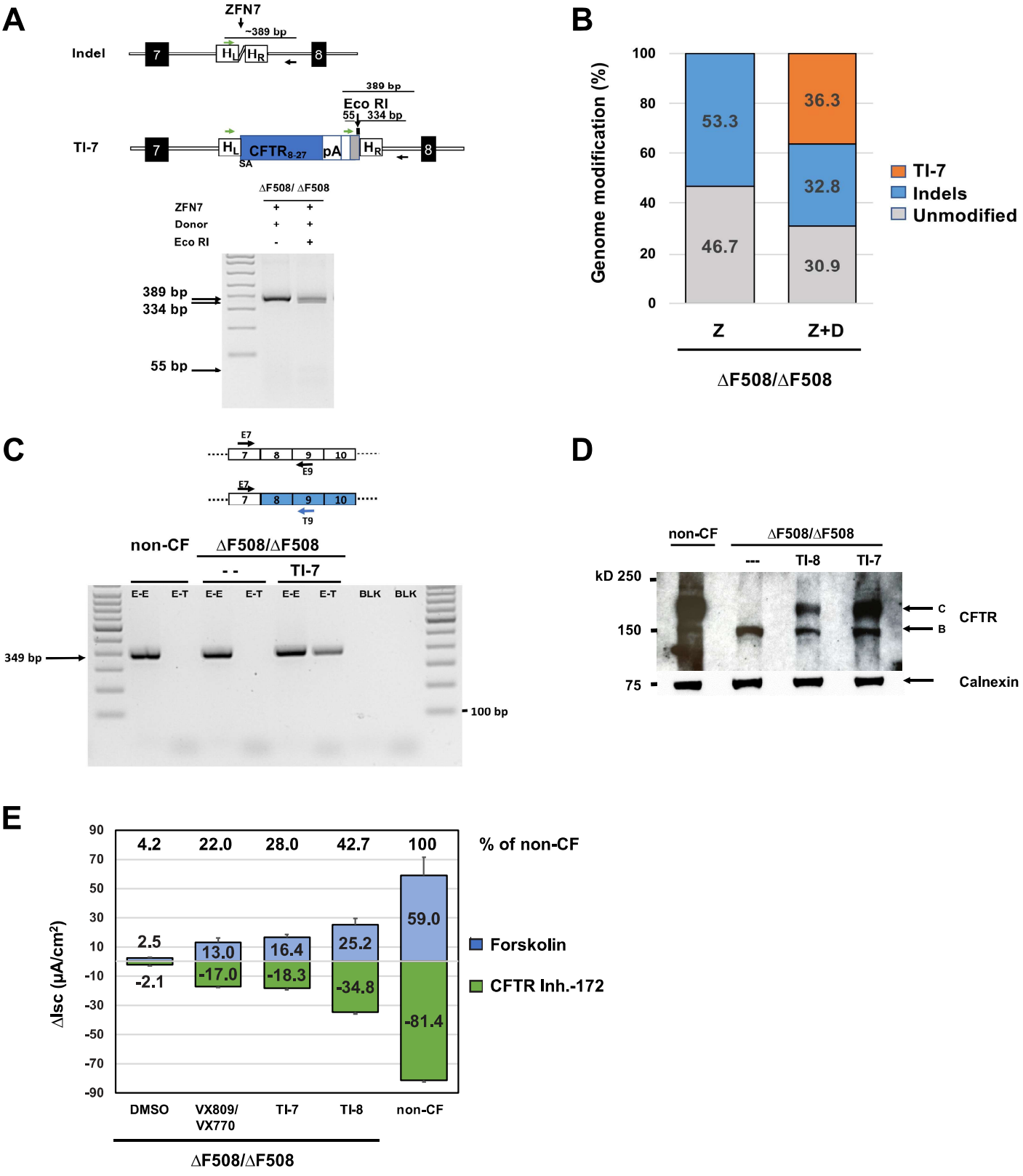
A
ZFN7
~389 bp
Indel
7
HL
HR
8
389 bp
Eco RI
55
334 bp
TI-7
CFTR8-27
SA
pA
ΔF508/ ΔF508
ZFN7
Donor
Eco RI
389 bp
334 bp
55 bp
B
Genome modification (%)
100
80
60
40
20
0
53.3
46.7
36.3
32.8
30.9
Z
Z+D
ΔF508/ΔF508
TI-7
Indels
Unmodified
C
E7
7
8
9
10
E9
T9
non-CF
ΔF508/ΔF508
- -
TI-7
E-E
E-T
BLK
349 bp
100 bp
D
non-CF
ΔF508/ΔF508

TI-8
TI-7
kD 250
150
75
C
B
CFTR
Calnexin
E
% of non-CF
4.2
22.0
28.0
42.7
100
90
70
50
30
10
-10
-30
-50
-70
-90
ΔIsc (μA/cm²)
2.5
-2.1
13.0
-17.0
16.4
-18.3
25.2
-34.8
59.0
-81.4
Forskolin
CFTR Inh.-172
DMSO
VX809/
VX770
TI-7
TI-8
non-CF
ΔF508/ΔF508

Fig. S7

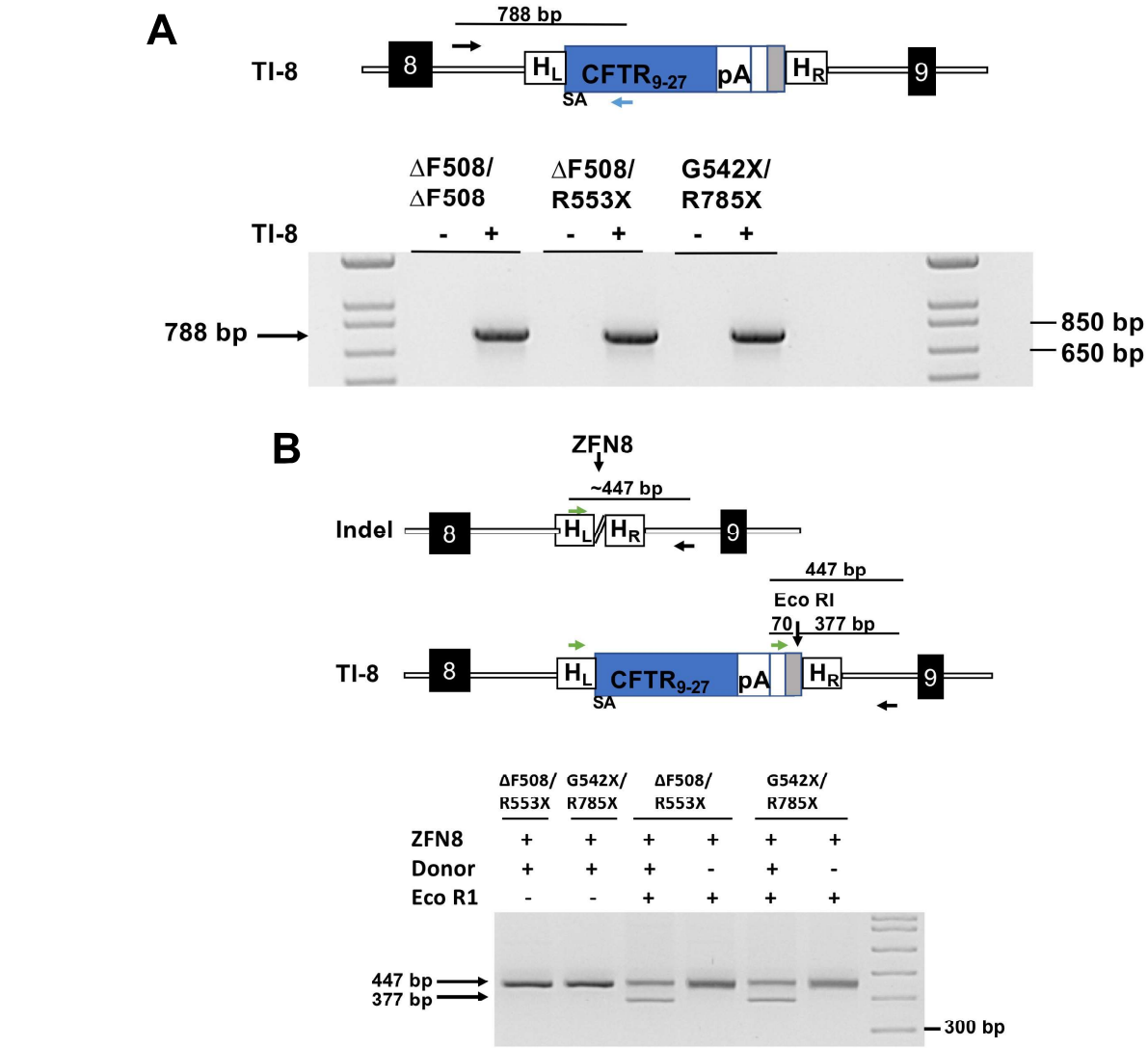
A
788 bp
TI-8
8
HL
CFTR9-27
pA
HR
9
SA
ΔF508/ ΔF508
ΔF508/ R553X
G542X/ R785X
TI-8
- + - + - +
788 bp
850 bp
650 bp
B
ZFN8
~447 bp
Indel
8
HL/HR
9
447 bp
Eco RI
70 377 bp
TI-8
8
HL
CFTR9-27
pA
HR
9
SA
ΔF508/ R553X
G542X/ R785X
ΔF508/ R553X
G542X/ R785X
ZFN8 + + + + + +
Donor + + + - + -
Eco R1 - - + + + +
447 bp
377 bp
300 bp

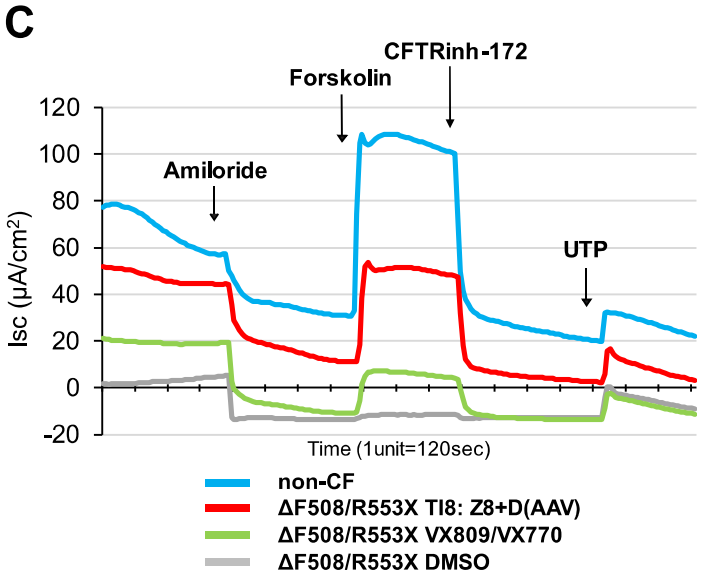
C
CFTRinh-172
Forskolin
Amiloride
UTP
120
100
80
60
40
20
0
-20
Isc (μA/cm²)
Time (1unit=120sec)
non-CF
ΔF508/R553X TI8: Z8+D(AAV)
ΔF508/R553X VX809/VX770
ΔF508/R553X DMSO

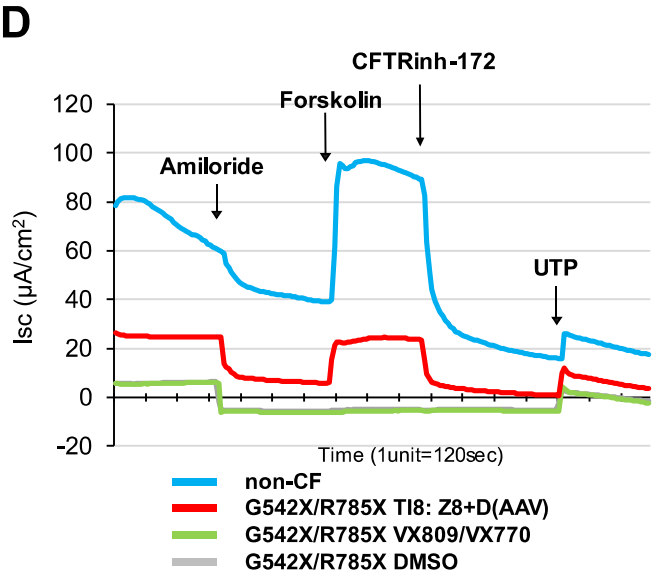
D
CFTRinh-172
Forskolin
Amiloride
UTP
120
100
80
60
40
20
0
-20
Isc (μA/cm²)
Time (1unit=120sec)
non-CF
G542X/R785X TI8: Z8+D(AAV)
G542X/R785X VX809/VX770
G542X/R785X DMSO

Fig. S8

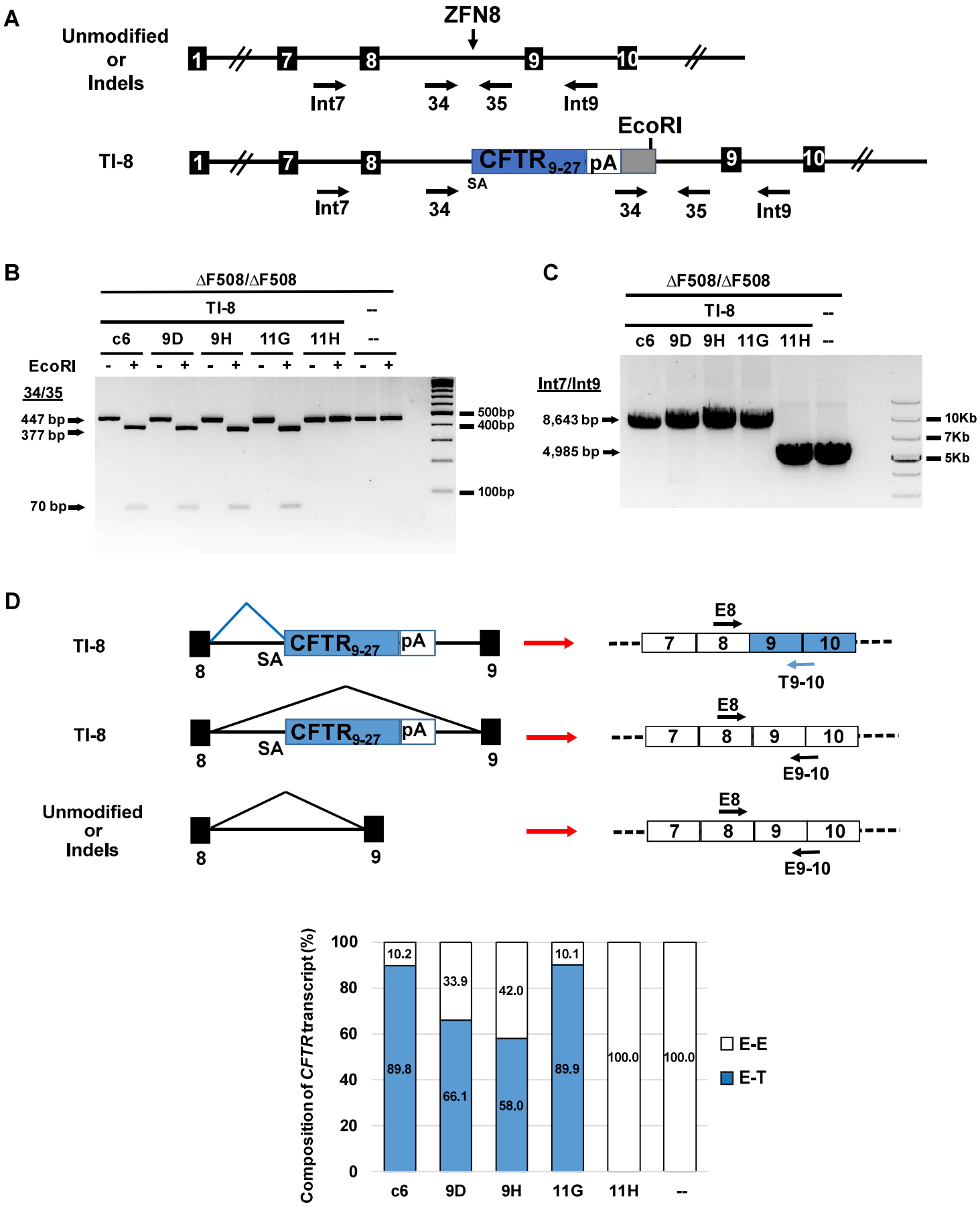
A
Unmodified or Indels
ZFN8
1
7
8
9
10
Int7
34
35
Int9
TI-8
EcoRI
CFTR9-27
pA
SA
34
35
B
ΔF508/ΔF508
TI-8
--
c6
9D
9H
11G
11H
--
EcoRI
- + - + - + - + - + - +
34/35
447 bp
377 bp
70 bp
500bp
400bp
100bp
C
ΔF508/ΔF508
TI-8
--
c6 9D 9H 11G 11H --
Int7/Int9
8,643 bp
4,985 bp
10Kb
7Kb
5Kb
D
TI-8
SA
CFTR9-27
pA
8
9
E8
7
8
9
10
T9-10
TI-8
E9-10
Unmodified or Indels
Composition of CFTR transcript (%)
100
80
60
40
20
0
10.2
89.8
33.9
66.1
42.0
58.0
10.1
89.9
100.0
100.0
c6
9D
9H
11G
11H
--
E-E
E-T

Fig. S9

A

OT#	Mock		Parent ZFNs			Improved ZFNs			Genome notes	Locus
	%Indels	#Seq reads	%Indels	Bonferroni P-value	#Seq reads	%Indels	Bonferroni P-value	#Seq reads		
On	0.0495	54497	97.6483	0	54131	97.8171	0	48835	*CFTR* intron 8 (on-target)	chr7:117541450-117541490
OT2	0.097	57721	9.7478	0	54966	0.293	9.466E-11	40612	Intergenic	chr18:1439142-1439182
OT3	0.2061	61150	1.8446	0	42666	0.2268	0.907	52465	Intergenic	chr11:116695570-116695610
OT4	0.0367	48996	0.6216	0	38929	0.0725	0.06811	34467	Intergenic	chr1:200488808-200488848
OT10	0.0653	52075	0.4425	0	42263	0.1016	0.07636	56127	*ASCL5* intron 1	chr1:201126946-201126986
OT12	0.0087	57288	0.4717	0	39004	0.1295	1.462E-10	39391	*SARS* intron 1	chr1:109214368-109214408
OT19	0.0726	23422	0.8946	0	17214	0.2504	0.00001905	19168	Intergenic	chr17:38257580-38257620
OT21	0.032	40583	0.2062	6.217E-15	50439	0.0422	0.9376	35529	*MTNR1A* intron 1	chr4:186554568-186554608
OT25	0.0224	44568	0.1152	9.259E-07	39939	0.0569	0.01642	47421	Intergenic	chr9:97789720-97789760
OT28	0.0484	80520	0.1754	2.219E-12	67858	0.0678	0.3134	53059	Intergenic	chr1:26966994-26967034
OT32	0.1038	85763	0.2097	0.00000141	62480	0.0657	1	71526	Intergenic	chr21:43502506-43502546

B

	Exp	%TI	%Indels	%Unmodified	#Seq reads
ZFN (2ug each)	1	0.00	94.55	5.45	43320
	2	0.00	94.57	5.43	49665
	3	0.11	94.69	5.20	51279
	mean±SD	0.0 ± 0.1	94.6 ± 0.1	5.36 ± 0.1	
ZFN (2ug each) AAV6 (MOI=1x10^6)	1	51.30	44.53	4.17	45639
	2	56.62	37.91	5.47	53656
	3	59.92	35.08	5.00	47649
	mean±SD	56.0 ± 4.4	39.2 ± 4.9	4.9 ± 0.7	

C

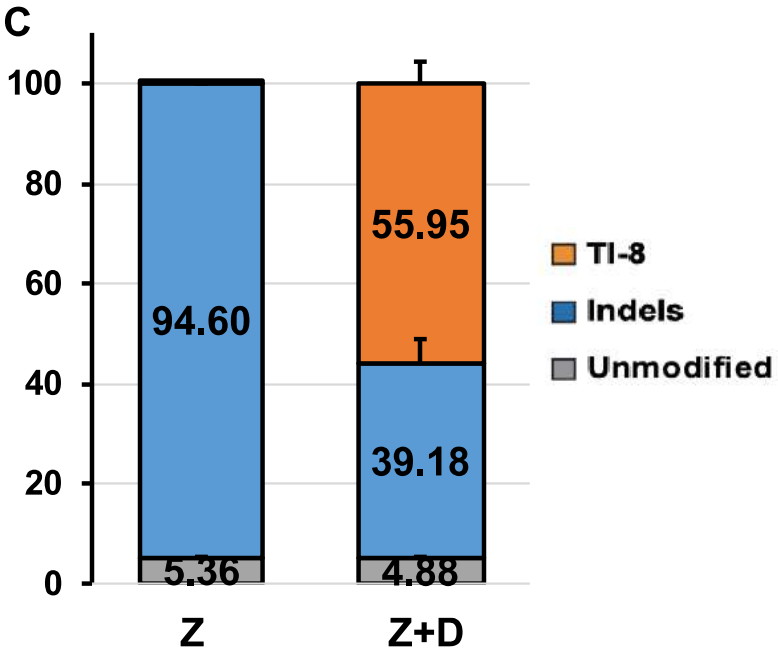

Supplemental Figure Captions

Fig. S1. Feeder-free expansion of primary airway basal cells. (A) Population doublings (PDs) for non-CF basal cells in two established airway basal cell culture conditions, PneumaCult™-Ex Plus Medium (P-ExPlus) and dual SMAD inhibition condition (SMADinh). Non-CF basal cells at passage 1 (p1) were plated with each media and each dot represents total PD from p1 to each passage (up to p12). **(B)** Flow cytometric analysis of cell surface markers CD49f and NGFR at the indicated passage numbers. **(C)** Immunofluorescence staining of acetylated tubulin (ACT) at 4 weeks of ALI culture at the indicated number of passages. Representative 40x images in whole mount staining are shown. Scale bar: 50μm. **(D)** Representative tracings (short circuit current) of cell monolayers at 4 weeks of ALI evaluated by Ussing chamber analysis; the passage numbers are as indicated. **(E)** Summary of CFTR chloride current stimulated by forskolin and inhibited by CFTR inhibitor-172 (CFTR inh-172) is plotted. Difference of Isc (Δlsc) ($\mu A/cm^2$) before and after stimulation or inhibition of CFTR are calculated from tracings represented by (D). (mean ± SD, n=4 technical replicates)

Fig. S2. Sequence-specific correction of ΔF508 mutation. (A) The ZFN11 left (L) and right (R) pair is designed to identify and cleave ΔF508 *CFTR* sequences in exon 11. ZFN-L targets ΔF508 (red box) while ZFN-R recognizes both *wt* and ΔF508 *CFTR*. ZFN recognition sequences are colored in orange for ZFN11-L and in blue for ZFN11-R (the nucleotides within ZFN11-L and ZFN11-R that are denoted in black are skipped bases). **(B)** The percent correction mediated by ZFN11 and ssDNA was assessed by the TIDER (Tracking of Insertions, DEletions and Recombination events) bioinformatics tool (https://tider.deskgen.com/) [1]. 2μg of each ZFN11 mRNA was co-electroporated with the 200-mer ssDNA. Increases in the correction efficiency were observed with increased amounts of ssDNA. **(C)** Total cell number (x 10^6) at 3 days post-electroporation for the experiment shown in panel B. **(D)** The percent correction mediated by ZFN11 and AAV-6 donor was assessed by TIDER. Transduction with 2 kb AAV-6 donor was performed immediately after electroporation of 2μg or 3μg of each ZFN11 mRNA. Correction efficiency plateaued for MOI=10^6 (10^6 vg/cell) or higher (mean ± SD, n=3 biological replicates).

Fig. S3. Gene editing methodology does not alter airway basal cell differentiation. Immunofluorescence staining for airway epithelium markers in ALI culture. ALI cultures were established from unmanipulated cells (ΔF508/ΔF508) or manipulated cells (Z+D(AAV)) in Fig. 2B. Major epithelial cell types were identified with markers: P63 for basal cell; MUC5AC for secretory cells; FOXJ1 for ciliated cells; FOXI1 for ionocytes. Representative 40x images in transverse section staining from three random fields in each biological replicate, experiment 1, 2 and 3. Scale bar: 50μm (Panels). % of indicated cell type (mean ± SD, n=3 biological replicates). ns, not significant (Two-tailed paired t-test) (Graphs).

Fig. S4. Sequence-specific ΔF508 correction restores fully glycosylated CFTR protein expression. Western blot of protein lysates harvested at 4 weeks of ALI culture of ΔF508/ΔF508 cells that were edited with ZFN11 together with either ssDNA or AAV-6 donors. Calnexin: loading control. The mature fully-glycosylated CFTR protein is identified as band C. For ZFN/ssDNA correction of ΔF508 (% correction: 10.6 ± 2.6) the level of restored CFTR band C was 68.2 ± 16.3% of total CFTR protein. For ZFN/AAV correction of ΔF508 (% correction: 31.0 ± 4.0) the level of restored CFTR band C was 95.3 ± 5.3% of total CFTR protein. We note that since the level of band B for ΔF508/ΔF508 cells is very low (likely reflecting degradation and absence of maturation), even modest rates of correction result in the fully glycosylated band C being the main form of CFTR protein.

Fig. S5. Efficient *SA-CFTR*$_{9\text{-}27}$*-pA* TI into *CFTR* intron 8 of ΔF508/ΔF508 airway basal cells. (A) Inside-outside PCR amplification at the 5' end of the targeted transgene at 4 days of genome editing. A 788 bp PCR fragment was amplified with one primer targeting inside of the codon-optimized sequence (blue arrow in the schematic) and another primer targeting outside of left homology arm (H_L) (Black). **(B)** Indel and TI-8 diagram showing *CFTR* intron 8 genomic organization. Horizontal arrows indicate the oligo priming sites, and expected PCR amplicon sizes are shown. Only when ZFN8 and AAV-6 donor were co-delivered did Eco RI cleave the 3' end 447 bp PCR amplicon, evidence for TI-8. **(C)** Representative tracings (Isc) of cell monolayers from 5 experimental conditions: DMSO-treated, VX-

809/VX-770 pre-treated, TI7: Z7+D-treated and TI8: Z8+D-treated CF (ΔF508/ΔF508), and non-CF evaluated by Ussing chamber analysis at 4 weeks of ALI culture.

Fig. S6. Efficient *SA-CFTR*$_{8\text{-}27}$*-pA* TI into *CFTR* intron 7 of ΔF508/ΔF508 airway basal cells. (A) Schematic of site-specific targeted editing of *CFTR* intron 7. Indel diagram shows *CFTR* genomic organization between exon 7 and 8 (black boxes) (not to scale). TI-7 diagram shows intron 7 TI of human codon optimized *CFTR*$_{8\text{-}27}$ cDNA preceded by a splice acceptor, followed by bovine growth hormone (bGH) pA sequence, and flanked by 246 bp homology left (H_L) and 271 bp homology right (H_R) intron 7 sequences. Horizontal arrows indicate oligos amplifying unmodified, indel or TI-7 events and used to quantify frequency of each by NGS. Lower gel shows evidence for TI-7 via Eco RI digestion. **(B)** The genome modification frequency determined by NGS for a TI-7 experiment. The efficiency was measured 4 days after the delivery of ZFNs targeting intron 7 (ZFN7) followed immediately by AAV-6 *CFTR*$_{8\text{-}27}$ cDNA donor. Z: ZFN7 alone (23,337 NGS reads), Z+D: ZFN7 and AAV-6 donor (29,843 NGS reads). **(C)** Detection of transgene *CFTR*$_{8\text{-}27}$ mRNA. Schematic of *CFTR* endogenous and transgene mRNA. RT-PCR with oligos E7 (endogenous exon 7) and T9 (transgene exon 9) showed the expected 349 bp amplicon only in the TI-7 ΔF508/ΔF508 sample, while PCR amplification with oligos E7 and E9 (endogenous exon 9) shows the expected 349 bp amplicon in all samples. **(D)** Restoration of fully glycosylated CFTR protein via TI-7. Western blot of protein lysates harvested at 4 weeks of ALI culture. CFTR band C is absent in ΔF508/ΔF508 cells, but restored for both TI-8 and TI-7 ΔF508/ΔF508. Calnexin: loading control. **(E)** Summary of CFTR function. Bulk TI-7 ΔF508/ΔF508 cells in ALI cultures showed the restoration of CFTR function measured as Δlsc ($\mu A/cm^2$) at levels similar to ΔF508/ΔF508 cells treated with VX-809/VX-770.

Fig. S7. Efficient TI of *SA-CFTR*$_{9\text{-}27}$*-pA* into *CFTR* intron 8 of ΔF508/R553X and G542X/R785X airway basal cells. The expected inside-outside PCR amplification at the 5' end **(A)** and Eco RI digestion of the 3' end PCR fragment **(B)** was present only in TI-8 ΔF508/R553X and TI-8 G542X/R785X basal cells. **(C, D)** Representative tracings (Isc) of cell monolayers with (C) ΔF508/R553X or (D) G542X/R785X *CFTR* genotypes. The following chronic treatments and experimental conditions were applied: DMSO-treated CF, VX-809/VX-770 pre-treated CF , or TI8: Z8+D-treated CF; a non-CF control was evaluated in parallel. Ussing chamber analysis was performed at 4 weeks of ALI culture.

Fig. S8. The majority of *CFTR* transcripts from TI-8 alleles incorporates the corrective transgene sequences. (A) Schematic of *CFTR* gene showing location of PCR primers employed for genotyping of edited single-cell derived clones. Primers are identified by black horizontal arrows. **(B)** Shown is the EcoRI digestion pattern for four homozygous TI-8 clones (c6, 9D, 9H and 11G), one non-TI clone (11H), and the parental ΔF508/ΔF508 cells. TI-8 is evidenced by EcoRI cleavage of the 447 bp PCR amplicon (primers 34/35); absence of the undigested 447bp band in the EcoRI treated lane is consistent with TI-8 homozygosity. **(C)** Homozygosity of the four clones (c6, 9D, 9H, 11G) was confirmed by PCR amplification (primers Int7/Int9): the presence of the 8.64 kb band is characteristic of TI-8 while the absence of a band at 4,99 kb (or similar size due to possibility of Indels) confirms TI-8 homozygosity. **(D)** Composition of transcripts from TI-8 alleles. Shown above are schematics of normal and alternate splicing of *CFTR* transcripts. The E8/E9-10 RT-PCR amplicon can either arise from a non-TI allele (unmodified or with indels) or from alternate splicing in a TI-8 allele from the endogenous exon 8 across the corrective transgene to the downstream endogenous exon 9. The E8/T9-10 RT-PCR amplicon reflects the desired splicing from endogenous exon 8 to the transgene exon 9. The reverse primer T9-10 recognizes only codon-optimized transgene at exon 9-10 junction (blue) while the reverse primer E9-10 recognizes the endogenous exon 9-10 junction (black). Either primer together with the forward primer E8 amplify a 139 bp RT-PCR amplicon used for absolute quantitative PCR. The graph shows the composition (E-E vs. E-T) of *CFTR* transcripts.

Fig. S9. Optimization of ZFN8 decreases off-target activity while maintaining efficient cleavage and TI at intron 8. (A) Examination, via deep sequencing, of previously identified off-target sites in basal cells treated with either parental or optimized ZFN8. Ten loci out of 31 candidates originally identified via unbiased genome-wide oligonucleotide capture in K562 cells (Table S4) yielded a statistically significant (Bonferroni P-value <0.05) level of

indels in ΔF508/ΔF508 basal cells electroporated with parental ZFN8 and only 4 loci yielded a statistically significant level of indels in optimized ZFN8 as compared to mock electroporated control basal cells. **(B and C)** Frequency of genome modification in ΔF508/ΔF508 basal cells utilizing the optimized ZFN8s followed by AAV-6 transduction of the *SA-CFTR*$_{9\text{-}27}$*-pA* donor. Editing events were categorized as corrected (TI-8), indels, or unmodified. Three individual experiments were performed (mean ± SD, n=3 biological replicates); mean values are presented in (C).

Table S1

	Exp	%Corrected	%Indels	%Unmodified	#Seq reads
ZFN (2μg each)	1	0.0	44.8	55.2	30662
	2	0.0	42.1	57.9	28668
	3	0.0	47.0	53.0	35480
	mean±SD	**0.0 ± 0.0**	**44.6 ± 2.4**	**55.4 ± 2.4**	
ZFN (2μg each) ssDNA (20μg)	1	13.0	53.0	34.1	19184
	2	11.1	47.3	41.7	24706
	3	7.9	52.8	39.3	28720
	mean±SD	**10.6 ± 2.6**	**51.0 ± 3.2**	**38.4 ± 3.9**	

	Exp	%Corrected	%Indels	%Unmodified	#Seq reads
ZFN (3μg each)	1	0.0	48.9	51.1	23589
	2	0.0	44.2	55.8	28238
	3	0.0	37.4	62.5	36707
	mean±SD	**0.0 ± 0.0**	**43.5 ± 5.7**	**56.5 ± 5.7**	
ZFN (3μg each) AAV (MOI=2x10^6)	1	34.9	20.2	45.0	31866
	2	31.2	21.5	47.3	23111
	3	26.9	17.6	55.4	30344
	mean±SD	**31.0 ± 4.0**	**19.8 ± 1.9**	**49.3 ±5.5**	

Table S2

A

	#inserts	Cell type		Forskolin		CFTR Inh.-172	
				ΔIsc(mean±SD)	%non-CF	ΔIsc(mean±SD)	%non-CF
	n=4	non-CF	no treatment	62.1 ± 12.5	100	-72.2 ± 12.4	100
	n=3	ΔF508/ΔF508	DMSO	3.6 ± 0.1	5.8	-2.6 ± 0.4	3.6
	n=4		VX809/VX770	13.2 ± 2.0	21.3	-19.2 ± 3.4	26.6
Exp. 1	n=4		ZFN+ssDNA	8.6 ± 0.9	13.8	-12.4 ± 1.8	17.2
Exp. 2	n=4		ZFN+ssDNA	9.9 ± 2.0	15.9	-13.9 ± 3.1	19.3
Exp. 3	n=4		ZFN+ssDNA	6.0 ± 1.0	9.7	-7.5 ± 0.6	10.4

	#inserts	Cell type		Forskolin		CFTR Inh.-172	
				ΔIsc(mean±SD)	%non-CF	ΔIsc(mean±SD)	%non-CF
Exp. 1	n=4	ΔF508/ΔF508	DMSO	1.0 ± 0.1	1.9	-0.6 ± 0.3	1.0
	n=4		VX809/VX770	12.3 ± 3.1	23.5	-15.8 ± 3.5	27.5
	n=4		ZFN+AAV	18.9 ± 0.6	36.1	-27.4 ± 1.4	47.7
Exp. 2	n=4	non-CF	no treatment	53.4 ± 1.9	100	-55.8 ± 9.0	100
	n=4	ΔF508/ΔF508	DMSO	1.1 ± 0.1	2.1	-0.4 ± 0.7	0.7
	n=4		VX809/VX770	13.9 ± 3.6	26.0	-17.9 ± 4.9	32.1
	n=4		ZFN+AAV	24.2 ± 1.1	45.3	-32.2 ± 2.8	57.7
Exp. 3	n=4	non-CF	no treatment	44.9 ± 3.4	100	-59.7 ± 7.7	100
	n=4	ΔF508/ΔF508	DMSO	1.3 ± 0.2	2.9	-0.1 ± 1.0	0.2
	n=4		VX809/VX770	13.7 ± 1.0	30.5	-20.6 ± 0.7	34.5
	n=4		ZFN+AAV	17.6 ± 0.8	39.2	-26.0 ± 1.4	43.6

B

#Biological replicates	Cell type		Forskolin		CFTR Inh.-172	
			ΔIsc(mean±SD)	%non-CF	ΔIsc(mean±SD)	%non-CF
n=1	non-CF	no treatment	62.1	100	-72.2	100
n=1	ΔF508/ΔF508	DMSO	3.6	5.8	-2.6	3.6
n=1		VX809/VX770	13.2	21.3	-19.2	26.6
n=3		ZFN+ssDNA	8.2 ± 2.0	13.2 ± 3.2	-12.4 ± 1.8	15.6 ± 4.6

#Biological replicates	Cell type		Forskolin		CFTR Inh.-172	
			ΔIsc(mean±SD)	%non-CF	ΔIsc(mean±SD)	%non-CF
n=3	non-CF	no treatment	50.2 ± 4.7	100.0 ± 0.0	-57.5 ± 4.6	100.0 ± 0.0
n=3	ΔF508/ΔF508	DMSO	1.1 ± 0.2	2.3 ± 0.5	-0.4 ± 0.2	0.6 ± 0.4
n=3		VX809/VX770	13.3 ± 0.9	26.7 ± 3.6	-18.1 ± 2.4	31.4 ± 3.6
n=3		ZFN+AAV	20.2 ± 3.5	40.2 ± 4.7	-57.7 ± 2.0	49.6 ± 7.3

Table S3

A

	Exp	ZFN	AAV(MOI)	%TI	%Indels	%Unmodified	#Seq reads
Z	1	2µg each	NA	0.0	86.9	13.1	8061
	2			0.0	92.4	7.6	8792
	3			0.0	77.8	22.2	17385
	4			0.0	90.0	10	14872
	5			0.0	85.4	14.6	21852
	mean±SD			0.0 ± 0.0	86.5 ± 5.6	13.5 ± 5.6	
Z+D (AAV)	1	2µg each	$2x10^6$	47.0	42.8	10.2	8245
	2		$6x10^6$	50.1	43.2	6.7	8427
	3		$2x10^6$	60.3	23.5	16.2	16136
	4		$2x10^6$	64.2	28.3	7.6	17218
	5		$2x10^6$	60.7	27.4	11.9	19226
	mean±SD			56.5 ± 7.4	33.0 ± 9.3	10.5 ± 3.8	

B

ΔF508/ΔF508	Exp 2	%TI	%Indels	%Unmodified	#Seq reads
ZFN (2µg each)	4 days	0.0	92.4	7.6	8792
ZFN (2µg each) AAV6 (MOI=$6x10^6$)		50.1	43.2	6.7	8427
ZFN (2µg each)	30 days ALI	0.0	94.0	6.0	8805
ZFN (2µg each) AAV6 (MOI=$6x10^6$)		43.9	47.3	8.9	9675

C

ΔF508/R553X	Exp	%TI	%Indels	%Unmodified	#Seq reads
ZFN (2µg each) AAV6 (MOI=$2x10^6$)	1	44.9	36.2	18.9	7964
	2	48.6	20.5	30.9	16218
	3	56.6	24.8	18.6	17894
	mean±SD	50.0 ± 6.0	27.2 ± 8.1	22.8 ± 7.0	

D

G542X/R785X	Exp	%TI	%Indels	%Unmodified	#Seq reads
ZFN (2µg each) AAV6 (MOI=$2x10^6$)	1	53.2	34.8	12.0	8395
	2	66.0	25.5	8.5	14035
	3	61.7	26.2	12.0	21710
	4	66.0	26.0	7.92	17329
	mean±SD	61.8 ± 6.0	28.1 ± 4.4	10.1 ± 2.2	

Table S4

OT#	Chromosome	Start(hg38)	End(hg38)	Oligo capture events
OT1	chr7	117541450	117541490	624
OT2	chr18	1439142	1439182	400
OT3	chr11	116695570	116695610	157
OT4	chr1	200488808	200488848	154
OT5	chr7	43884378	43884418	22
OT6	chr2	172021700	172021740	21
OT7	chrX	156024044	156024084	20
OT8	chrY	57210564	57210604	20
OT9	chr1	186506	186546	19
OT10	chr1	201126946	201126986	19
OT11	chr12	16100	16140	19
OT12	chr1	109214368	109214408	18
OT13	chr15	101974938	101974978	17
OT14	chr16	15668	15708	16
OT15	chr2	30481092	30481132	16
OT16	chr4	39348778	39348818	16
OT17	chr9	16096	16136	16
OT18	chr1	15984	16024	15
OT19	chr17	38257580	38257620	15
OT20	chr17	47530832	47530872	15
OT21	chr4	186554568	186554608	14
OT22	chr2	113597412	113597452	12
OT23	chr6	13274234	13274274	12
OT24	chrX	101803712	101803752	12
OT25	chr9	97789720	97789760	12
OT26	chr12	54698438	54698478	11
OT27	chr17	38677118	38677158	10
OT28	chr1	26966994	26967034	9
OT29	chr3	90645844	90645884	7
OT30	chr3	90645930	90645970	7
OT31	chr6	5711448	5711488	7
OT32	chr21	43502506	43502546	7

Table S5

Primary antibody

Target	Host	Cat#	Manufacturer	Purpose	Dilution
CFTR	Mouse IgG2b	A4, 596	Cystic Fibrosis Foundation	Western Blot	1:1000
Calnexin	Rabbit polyclonal	ab22595	Abcam	Western Blot	1:5000
FOXJ1	Mouse monoclonal IgG1	14996580	Invitrogen	IF	1:200
FOXI1	Rabbit polyclonal IgG	HPA071469	Sigma	IF	1:200
Acetylated Tubulin	Mouse monoclonal IgG2b	T7451	Sigma	IF	1:1000
TP63 (N2C1)	Rabbit polyclonal IgG	GTX102425	GeneT ex	IF	1:100
TP63 (4A4)	Mouse monoclonal IgG2a/kappa	CM163A	Biocare	IF	1:100
MUC5AC (45M1)	Mouse monoclonal IgG1-kappa	MS-145-PO	Thermo	IF	1:200
MUC5AC (E309I)	Rabbit monoclonal IgG	61193	CST	IF	1:200
Keratin 5 (Poly19055)	Rabbit polyclonal	905501	Biolegend	IF	1:200
Keratin 5 (D4U8Q)	Rabbit monoclonal IgG	25807	CST	IF	1:200
CD49f, PE	Rat monoclonal IgG2a, κ	313612	Biolegend	Flow Cyt	1:50
CD271 (NGFR), APC	Mouse monoclonal IgG1	345108	Biolegend	Flow Cyt	1:50

Secondary antibody

Name	Cat#	Manufacturer	Purpose	Dilution
HRP-linked horse anti-mouse IgG	7076S	CST	Western Blot	1:5000
HRP-linked goat anti-rabbit IgG	ab205718	Abcam	Western Blot	1:20000
Alexa Fluor Plus 555 Donkey anti-Rabbit IgG (H+L)	A32794	Invitrogen	IF	1:500
Alexa Fluor 488 Donkey anti-mouse IgG (H+L)	A21202	Invitrogen	IF	1:500
Alexa Fluor 555 Goat anti-Mouse IgG (H+L)	A21424	Invitrogen	IF	1:500
Alexa Fluor 488 F(ab')2-Goat anti-Mouse IgG (H+L)	A11017	Invitrogen	IF	1:500

Table S6

Name	5' to 3'	purpose
CFaav2kbFw	ATAAGAATGCGGCCGCCCTCTGCTACCTCCTTTCCTT	2kb CFTR AAV6 construct
CFaav2kbRv	ATAAGAATGCGGCCGCATCTAATCCACGGTTTGCCC	2kb CFTR AAV6 construct
CFi10aFw	AGTCTATATTTGTTTTCCAGTGGC	Amplification of targeted region
CFi11aRv	TCCGCAACTTTTCCACTCGTA	Amplification of targeted region
CF5	CATTCACAGTAGCTTACCCA	Sanger sequencing
Miseq-e11-Fw	GGGAGAACTGGAGCCTTCAG	MiSeq Exon11
Miseq-e11-Rv	GTAGTGTGAAGGGTTCATATGC	MiSeq Exon11
CF34f	GCAAGGCAAGGACCAGGC	EcoR1 TI-8
CF35r	GCCAAGCACTAGGATTCATCAT	EcoR1 TI-8
CF36f	GGATGGTGTCAATATGGGTTATG	EcoR1 TI-7
CF37r	CTCTGATATCCTTGTCATCACCC	EcoR1 TI-7
72CF-wtE8f	GAAGGCAGCCTATGTGAGATAC	RT-PCR TI-8
81CF-wtE9r	CAATGTCTTATATTCTTGCTTTTGTA	RT-PCR TI-8
81CF-optE9r	GTACTCCTGCTTCTGCAGGAAGT	RT-PCR TI-8
70CF-wt7f	AGCTGGGAAGATCAGTGAAAG	RT-PCR TI-7
81CF-wtE9r	CAATGTCTTATATTCTTGCTTTTGTA	RT-PCR TI-7
81CF-optE9r	GTACTCCTGCTTCTGCAGGAAGT	RT-PCR TI-7
Miseq-i8-Fw (CF34f)	GCAAGGCAAGGACCAGGC	MiSeq intron 8
Miseq-i8-Rv	GAAGGGCTCTATTAGAGACTCC	MiSeq intron 8
Miseq-i7-Fw	GAGGTACCATTTTGGATGGTG	MiSeq intron 7
Miseq-i7-Fw	CAGGTGAGCAATAATGTTTGGG	MiSeq intron 7
CF41f	AGAGGTTGCAAATGGTGTCC	Clone genotype
CFintron7f	GAGTCCCTCTTAGTTCTGCAC	Clone genotype
CFintron9r	GTCCAGGTGCTAACAAAACTCAG	Clone genotype
WTex8 qPCRf	TATGACTCTCTTGGAGCAATAAAC	Quantitative RT-PCR TI-8
WTex9-10 qPCRr	ATTCCCCAAATCCCTCCTCC	Quantitative RT-PCR TI-8
optex9-10r	ACTCTCCGAAGCCTTCCTCC	Quantitative RT-PCR TI-8

Table S7

index	fragment ends	sample name	number of mapped read pair
AH756	paired end sequencing	Non-CF ALI	46271019
AH757	paired end sequencing	CF ALI	45444368
AH758	paired end sequencing	TI-8 CF ALI	37920997
AH774	paired end sequencing	Non-CF ALI	43663380
AH775	paired end sequencing	CF ALI	40605607
AH776	paired end sequencing	TI-8 CF ALI	29903855

Supplemental Table Captions

Table S1. Sequence-specific correction of ΔF508 mutation. Percentage of genome modification analyzed by NGS. Editing events were categorized as corrected, indels, or unmodified. Three individual experiments were performed (mean ± SD, n=3 biological replicates) and mean values are presented in Fig. 2B.

Table S2. Sequence-specific *Δ*F508 correction restores CFTR function. (A) CFTR chloride current stimulated by forskolin and inhibited by CFTR inhibitor-172 (CFTR inh-172). Mean values are obtained from 3 to 4 inserts as indicated (mean ± SD, n=3 or 4 technical replicates). **(B)** The average of indicated biological replicates, experiment 1, 2 and 3 in (A) (mean ± SD, n=3 biological replicates). Bottom half of table is presented in Fig. 2F.

Table S3. Efficient TI of *SA-CFTR*$_{9\text{-}27}$*-pA* into *CFTR* intron 8 in CF airway basal cells

Frequency of intron 8 genome modification in ΔF508/ΔF508 (A, B), ΔF508/R553X (C), and G542X/R785X basal cells (D) as determined by NGS. Editing events were characterized as corrected, indels, or unmodified. Mean and SD are shown where the biological experiments were independently replicated (n=3 to 5).

Table S4. Unbiased identification of potential off-target genome modification sites by ZFN8. A panel of 31 candidate top off-target sites (designated "OT2" through "OT32") was identified via unbiased oligonucleotide capture studies of the lead pair of ZFNs targeting human *CFTR* intron 8 in K562 cells. The top scored site of oligonucleotide capture was the intended on-target site within *hCFTR* intron 8 (hg38 coordinates chr7:117541450-117541490), which was designated "OT1".

Table S5. List of antibodies.

Table S6. List of oligos.

Table S7. Number of sequencing reads in ATAC-seq experiments.

Donor DNA sequences

200-mer ssODN (5'-3'): Site-specific ΔF508 correction

tcagagggtaaaattaagcacagtggaagaatttcattctgttctcagttttcctggattatgcctggcaccattaaagaaaatatc
atctttggtgtttcctatgatgaatatagatacagaagcgtcatcaaagcatgccaactagaagaggtaagaaactatgtgaaaact
ttttgattatgcatatgaacccttca

2 kb *wtCFTR* AAV donor DNA (From 5'ITR through 3'ITR): Site-specific ΔF508 correction

cctgcaggcagctgcgcgctcgctcgctcactgaggccgcccgggcgtcgggcgacctttggtcgcccggcctcagtgagcgagcga
gcgcgcagagagggagtggccaactccatcactaggggttcctgcccatggatttaaattctagaaggcctgcggccgcatctaatc
cacggtttgccctttccatttttttggatactgtattttaagctacattttactttctctgcaatttttttcataaaagattatat
aaaggaattgcaaatgccaactatcaaagatattgcttttgaatcacaaacactatttggagtatactgtcaataaacttcatagta
acatattccctgccctaacatttacagcaataactactgaacccaccatcacacaatttacatagtgaacagcacaagatccatata
ctggtttctcttggaatacttcatgtaattttcagataattagctcattctccaatattgttgtgaaatgagtaatgacatcatctt
catttgcctctgcatcaaagaattgcagtcactagaagttatatggtatttgttcaaagccagggatacaatatcttcacaatttt
acccctctaattctctgctggcagatcaatgctcattccattaggctatagtattattaaaattattaaaataatcttaataatttt
tggagtatatttttaaagatgcatattttgtggtatcttttaaaaagataccacatatcacttatatgcatgccatataaataacca
ttgaggacgtttgtctcactaatgagtgaacaaaattctcaccatttcataaaatgcatttattgtgatcaaatgaacccattattt
aaaaaataaattgcatttatttcatgtgtttgcaagcttcttaaagcataggtcatgtgttttattaattgatccattcacagtagc
ttacccatagaggaaacataaatatatgtagactaaccgattgaatatggagccaaatatataatttgggtagtgtgaagggttcat
atgcataatcaaaaagttttcacatagtttcttacctcttctagttggcatgctttgatgacgcttctgtatctatattcatcatag
gaaacaccaaagatgatattttctttaatggtgccaggcataatccaggaaaactgagaacagaatgaaattcttccactgtgctta
attttaccctctgaaggctccagttctcccataatcaccattagaagtgaagtctggaaataaaacccatcattattaggtcattat
caaatcacgctcaggattcacttgcctccaattatcatcctaagcagaagtgtatattcttatttgtaaagattctattaactcatt
tgattcaaaatatttaaaatacttcctgtttcaggtactctgctatgcacaaaagatacaagggaaagtaaaagagacaattacaat
acagtgtgacaagtattatgatagaggttcacagagaaggggcacatgattcagatagttggaataggtttggaggaagaatgggaa
aggttagtaacagctaacagttgccaagtgctcactctgtgtcgagtgctgttctatgtgctttaactatattaatttatttaatct
tcacagaaatcctacaaagtagattaccttcatattattaggtacagattaagtaatagagacatattcaggtaatattgttcccat
gagcctttcttggagtataaagtcatttaagagatgatagtacaaaaggactatcagtgaacaaagatttatataactgtgaacaaa
aattaaaactaatggcagaattcgagttgaaaaacaaagtttaaatatgttatatgtcctgacaataagaaaagttagaagtaaaaa
ccaaataaacaaacaaaggaaatggggtataagtgtggagtgtaaaggaaatttgctgattgctttattaagaaaagctgaaagtca
aaaggtatcatttaaagctaataaataaagtaatagaagcataagcagatttaacaatacaaagataaatctgaaaaaagataatac
tactgactaaaactgagtagaaggaaaggaggtagcagagggcggccgcaggaacccctagtgatggagttggccactccctctctg
cgcgctcgctcgctcactgaggccgggcgaccaaaggtcgcccgacgcccgggctttgcccgggcggcctcagtgagcgagcgagcg
cgcagctgcctgcagg

hCFTR_intron_7_AAV donor DNA (From 5'ITR through 3'ITR): Targeted Integration intron 7

cctgcaggcagctgcgcgctcgctcgctcactgaggccgcccgggcgtcgggcgacctttggtcgcccggcctcagtgagcgagcga
gcgcgcagagagggagtggccaactccatcactaggggttcctgcggccgcacgcgtgggcaaaatataaactacagcatttctgta
gcaatgagaccatttttcttcagttgagctccatgttctacaaacttcaatcaaaaaaggttctaggagactcagtgaaagttgata
cactgttcaaggaacaaataatttcagcacatgggaatttcacagggaaaaatatactaaaaagagaggtaccattttggatggtgt
caatatgggttatgaggaattcaggctgctgagtccagtgtaggatccctgacctcttctcttcctcccacagaacagaactgaagc
ttacccggaaggccgcctacgtgcggtacttcaacagcagcgccttcttcttctccggattcttcgtggtgttcctttccgtgttgc
cttacgcgctcattaaggggatcatcctgcggaagattttcaccacgatttccttctgcatcgtgctgaggatggccgtgactcggc
agttcccgtgggcagtccagacgtggtacgattccctgggcgccatcaacaagattcaggacttcctgcagaagcaggagtacaaga
ccttggagtacaatctcactactactgaagtggtcatggagaacgtgaccgcattttgggaggaaggcttcggagagttgttcgaaa
aggccaagcagaacaacaacaacagaaagacctccaatggcgatgattccctttttcttctccaatttctcccttcttggcactccgg
tgctcaaggatatcaatttcaaaatcgaacgcggacagctgctggcggtggcgggatcgaccggagctggaaagactagcctgctta
tggtcatcatgggagaactggagccttccgagggaaagattaagcactccggtcgcatcagcttttgttcccaattttcgtggatta
tgccgggaaccatcaaggaaaacattatcttcggggtgtcatacgacgagtaccgataccgcagcgtgatcaaggcctgccagctgg
aggaggacatctcgaaattcgccgaaaaggacaacattgtcctgggcgaaggtggcatcaccctctcgggcggacagcgcgcgagaa
tctccctggcccgcgcagtctacaaggatgccgatctgtacctcctggattccccgttcggctatctggacgtcctgaccgaaaagg
aaattttcgagtcgtgcgtctgcaagctcatggccaacaagacccgcatcctcgtcacctcgaagatggaacacctcaagaaggcag
acaagatccttatcctgcacgagggctcctcctacttctacggaaccttctccgagctgcagaacctccagcccgatttcagcagca
agctgatgggctgcgacagcttcgaccagttctcggccgaaagaagaaactcgattctgaccgaaaccctgcatagattctccctgg
aggggatgcgcccgtgtcctggaccgaaacgaagaagcagtcattcaagcaaaccggagagttcggcgaaaagcggaaaaactcga
tccttaacccgattaactccatccgcaagttctcaattgtgcaaaagacacccctgcaaatgaacggcatcgaagaggactccgacg
aacctctggaacggcggctgtcgctggtgcccgacagcgagcagggagaagccatcctcccccggatttccgtgatcagcactggcc
cgactctgcaagcccggcgccggcagtccgtgctgaacctgatgactcacagcgtgaaccagggccagaacatccatcgcaagacca
ccgccagcaccagaaaggtgtcgctggcgccccaagcaaacctgactgagcttgacatctactcgcgccggctctctcaagaaaccg
gtctggagatttcagaagaaattaacgaagaagatctgaaggaatgtttttcgacgatatggagtcaattccagctgtgactacct
ggaacacctacttgcgctacattaccgtccacaaatccttgatctttgtcctgatctggtgcctcgtgattttcctggccgaagtgg
ccgcatcgctcgtcgtgctgtggcttttggggaacacccccctgcaagacaaggggaacagcacccactcccggaacaattcttacg
ctgtgattatcacctccacgagcagctactacgtgttctacatctacgtgggcgtggccgatactcttctcgctatgggattcttcc
gcggtctgccgctggtgcatactctcatcaccgtgtccaagatcctgcaccacaagatgctgcactccgtcctgcaagcaccgatga
gcacactcaacaccctgaaggccggagggattcttaaccggttctccaaggacattgcaatcctggacgacctcctgccactgacca
tcttcgattttatccagttgctgctcatcgtgattggagccatcgcagtggtggccgtgctgcagccctacatcttcgtggcgactg
tgccggtcatcgtggccttcatcatgttgcgggcctacttcctgcaaactagccaacagctgaagcagctggagtccgaaggaagat
cgcctatctttacgcatcttgtgacctccttgaagggtctgtggaccctcagagccttcggacggcagccttatttcgaaactctgt
tccacaaggccctgaatctgcacaccgcgaactggttcctctatctgtcgaccctgcggtggtttcagatgaggatcgaaatgatct
tcgtgatcttcttcatcgccgtcaccttcatctccatcctcaccaccggagaaggcgaaggacgcgtgggaatcatcctgaccctgg
cgatgaacatcatgtccactctgcaatgggccgtcaactcctcgattgatgtggactctctgatgcgttccgtgtcaagggtgttca
agttcattgacatgcccactgagggaaaacctaccaagtccactaagccttacaagaacgggcagctgagcaaagtcatgattattg
agaacagccacgtcaagaaggacgacatctggccttccggaggacagatgaccgtgaaggatttgaccgccaagtacactgagggag
gaaacgcaatcctggagaacattagcttctccatctcgcctggccagcgcgtgggactgttgggcaggactggctccggcaaaagca
ccctcttgtcggccttcctgcgcctcctgaataccgaaggagagatccagatcgatggggtgtcttgggactcaatcactctgcagc
agtggcgcaaggcttttggcgtgattccgcagaaggtgttcatcttctcggggaccttccgcaagaacctcgacccctacgagcagt
ggtccgatcaggaaatctggaaggtggccgacgaggtcggcctccgttccgtgatcgagcaattccctggaaaactggacttcgtgc
tggtcgacggcggatgcgtgctgtcccacgggcacaagcaactgatgtgtcttgcccggagcgtgctcagcaaggccaagattcttc
tgctggacgagccatccgcccacctggaccccgtgacctaccagatcatccggcgcaccctgaagcaggccttcgcggactgcacag
tgattctgtgcgagcatcgcatcgaagcgatgctggagtgccagcagttcctggtcatcgaggagaacaaagtccggcaatacgaca
gcatccagaagctgctgaacgaacggtcgctgtttaggcaggccatctcaccaagcgaccgcgtgaagctgttcccccaccgcaaca
gcagcaagtgcaaatcaaagccgcagattgcggcgcttaaggaggagactgaagaagaagtccaagacaccaggctgtagctcgagc
tgtgccttctagttgccagccatctgttgtttgcccctcccccgtgccttccttgaccctggaaggtgccactcccactgtcctttc
ctaataaaatgaggaaattgcatcgcattgtctgagtaggtgtcattctattctgggggggtggggtggggcaggacagcaaggggga
ggattgggaagacaatagcaggcatgctggggatgcggtgggctctatccatggggatggtgtcaatatgggttatgcatgtacctg
ggctggaaaggaactgaattctggaaactgagctgcaggtgtgtgattgtaacaacaaaagaaatgctgaaatattaagtcctttgc
catgtaaatagaaaaagagtatttatttcccaaacattattgctcacctgtttttgttatgcctttcaagataaatccaggaaagga
attgcattttctttccagaaaacaagttcttgggggaattgttcaattggtagatgttgtttttctcattaacaagtgagtgctcca
tcacacttgctgagtgctccatcacacttgcggtaaccacgtgcggaccgagcggccgcaggaacccctagtgatggagttggccac
tccctctctgcgcgctcgctcgctcactgaggccgggcgaccaaaggtcgcccgacgcccgggctttgcccgggcggcctcagtgag
cgagcgagcgcgcagctgcctgcagg

hCFTR_intron_8_AAV donor DNA (From 5'ITR through 3'ITR): Targeted Integration intron 8

cctgcaggcagctgcgcgctcgctcgctcactgaggccgcccgggcgtcgggcgacctttggtcgcccggcctcagtgagcgagcga
gcgcgcagagagggagtggccaactccatcactaggggttcctgcggccgcacgcgtatttagacaaagtggtgaatctagctctga
atcatagtaagtagctctgggaatcatcttgtcttctgttagcccattgagagagaaatagagagagagagagagagaaagaaagaa
gaagaaacagatctggggagagtcactgaatgggagcatagagacagagaaacagatctagaaaaccaaactgggagaaaatgagag
aaaccaaaagagaggtagagaggagcagagaagaaaatgaagaagcaaggcaaggaccaggcttttcattatttcttatggccaag
acttcagtatgcgtggacttaaggatccctgacctcttctcttcctcccacaggacttcctgcagaagcaggagtacaagaccttgg
agtacaatctcactactactgaagtggtcatggagaacgtgaccgcattttgggaggaaggcttcggagagttgttcgaaaaggcca
agcagaacaacaacaacagaaagacctccaatggcgatgattccctttttcttctccaatttctcccttcttggcactccggtgctca
aggatatcaatttcaaaatcgaacgcggacagctgctggcggtggcgggatcgaccggagctggaaagactagcctgcttatggtca
tcatgggagaactggagccttccgagggaaagattaagcactccggtcgcatcagcttttgttcccaattttcgtggattatgccgg
gaaccatcaaggaaaacattatcttcggggtgtcatacgacgagtaccgataccgcagcgtgatcaaggcctgccagctggaggagg
acatctcgaaattcgccgaaaaggacaacattgtcctgggcgaaggtggcatcaccctctcgggcggacagcgcgcgagaatctccc
tggcccgcgcagtctacaaggatgccgatctgtacctcctggattccccgttcggctatctggacgtcctgaccgaaaaggaaattt
tcgagtcgtgcgtctgcaagctcatggccaacaagacccgcatcctcgtcacctcgaagatggaacacctcaagaaggcagacaaga
tccttatcctgcacgagggctcctcctacttctacggaaccttctccgagctgcagaacctccagcccgatttcagcagcaagctga
tgggctgcgacagcttcgaccagttctcggccgaaagaagaaactcgattctgaccgaaaccctgcatagattctccctggaggggg
atgcgcccgtgtcctggaccgaaacgaagaagcagtcattcaagcaaaccggagagttcggcgaaaagcggaaaaactcgatcctta
acccgattaactccatccgcaagttctcaattgtgcaaaagacacccctgcaaatgaacggcatcgaagaggactccgacgaacctc
tggaacggcggctgtcgctggtgcccgacagcgagcagggagaagccatcctcccccggatttccgtgatcagcactggcccgactc
tgcaagcccggcgccggcagtccgtgctgaacctgatgactcacagcgtgaaccagggccagaacatccatcgcaagaccaccgcca
gcaccagaaaggtgtcgctggcgccccaagcaaacctgactgagcttgacatctactcgcgccggctctctcaagaaaccggtctgg
agatttcagaagaaattaacgaagaagatctgaaggaatgtttttcgacgatatggagtcaattccagctgtgactacctggaaca
cctacttgcgctacattaccgtccacaaatccttgatctttgtcctgatctggtgcctcgtgattttcctggccgaagtggccgcat
cgctcgtcgtgctgtggcttttggggaacacccccctgcaagacaaggggaacagcacccactcccggaacaattcttacgctgtga
ttatcacctccacgagcagctactacgtgttctacatctacgtgggcgtggccgatactcttctcgctatgggattcttccgcggtc
tgccgctggtgcatactctcatcaccgtgtccaagatcctgcaccacaagatgctgcactccgtcctgcaagcaccgatgagcacac
tcaacaccctgaaggccggagggattcttaaccggttctccaaggacattgcaatcctggacgacctcctgccactgaccatcttcg
attttatccagttgctgctcatcgtgattggagccatcgcagtggtggccgtgctgcagccctacatcttcgtggcgactgtgccgg
tcatcgtggccttcatcatgttgcgggcctacttcctgcaaactagccaacagctgaagcagctggagtccgaaggaagatcgccta
tctttacgcatcttgtgacctccttgaagggtctgtggaccctcagagccttcggacggcagccttatttcgaaactctgttccaca
aggccctgaatctgcacaccgcgaactggttcctctatctgtcgaccctgcggtggtttcagatgaggatcgaaatgatcttcgtga
tcttcttcatcgccgtcaccttcatctccatcctcaccaccggagaaggcgaaggacgcgtgggaatcatcctgaccctggcgatga
acatcatgtccactctgcaatgggccgtcaactcctcgattgatgtggactctctgatgcgttccgtgtcaagggtgttcaagttca
ttgacatgcccactgagggaaaacctaccaagtccactaagccttacaagaacgggcagctgagcaaagtcatgattattgagaaca
gccacgtcaagaaggacgacatctggccttccggaggacagatgaccgtgaaggatttgaccgccaagtacactgagggaggaaacg
caatcctggagaacattagcttctccatctcgcctggccagcgcgtgggactgttgggcaggactggctccggcaaaagcaccctct
tgtcggccttcctgcgcctcctgaataccgaaggagagatccagatcgatggggtgtcttgggactcaatcactctgcagcagtggc
gcaaggcttttggcgtgattccgcagaaggtgttcatcttctcggggaccttccgcaagaacctcgacccctacgagcagtggtccg
atcaggaaatctggaaggtggccgacgaggtcggcctccgttccgtgatcgagcaattccctggaaaactggacttcgtgctggtcg
acggcggatgcgtgctgtcccacgggcacaagcaactgatgtgtcttgcccggagcgtgctcagcaaggccaagattcttctgctgg
acgagccatccgcccacctggaccccgtgacctaccagatcatccggcgcaccctgaagcaggccttcgcggactgcacagtgattc
tgtgcgagcatcgcatcgaagcgatgctggagtgccagcagttcctggtcatcgaggagaacaaagtccggcaatacgacagcatcc
agaagctgctgaacgaacggtcgctgtttaggcaggccatctcaccaagcgaccgcgtgaagctgttcccccaccgcaacagcagca
agtgcaaatcaaagccgcagattgcggcgcttaaggaggagactgaagaagaagtccaagacaccaggctgtagctcgagctgtgcc
ttctagttgccagccatctgttgtttgcccctcccccgtgccttccttgaccctggaaggtgccactcccactgtcctttcctaata
aaatgaggaaattgcatcgcattgtctgagtaggtgtcattctattctgggggggtggggtggggcaggacagcaagggggaggattg
ggaagacaatagcaggcatgctggggatgcggtgggctctatccatgggcaaggcaaggaccaggcttgttactgtaatacttctgt
tgcctctaattctctttaggtataggaattcccttatgctcctaccttcccctagggaaactgatttggagtctctaatagagcccttt
cttttagaatcacagtttgatgccttaaaactagttatatacccttcacatgcttccttaacccacagaagtgatgctaatgaggccc
ttaataaggagcgtgctattaagatgaagacattcatttttttttctccgtccaatgttggattaaggcacattagtgggtaattcag
ggttgctttgtaaattcatcactaaggttagcatgtaatagtacaaggaagaatcagttgtatgttaaatctaatgtataaaaagtt
ttataaaatatcatatgtttagagagtatatttcggtaaccacgtgcggaccgagcggccgcaggaacccctagtgatggagttggc
cactccctctctgcgcgctcgctcgctcactgaggccgggcgaccaaaggtcgcccgacgcccgggctttgcccgggcggcctcagt
gagcgagcgagcgcgcagctgcctgcagg

Supplemental Materials and Methods

Culture of airway basal cells: CF and non-CF airway epithelial cells, coded as KK003K (ΔF508/ΔF508 *CFTR*), KK002C (ΔF508/R553X *CFTR*), KKD023N (G542X/R785X *CFTR*) and DD023J (non-CF), were obtained from the CF cell core facility at the University of North Carolina, NC, USA. Two culture media were used for airway basal cells culture in this study. One was Pneumacult™-Ex Plus (STEMCELL technologies, Vancouver, Canada) medium; the other was dual SMAD inhibition medium consisting of SAGM™ medium (Lonza, Basel, Switzerland) supplemented with 10 µM RhoA kinase (ROCK) inhibitor Y27362 (Reagents Direct, Encinitas), 1 µM A-8301 (R&D Systems, Minneapolis, MN), 1 µM DMH-1 (R&D Systems) and 1 µM CHIR99021 (R&D Systems)[2]. In both culture conditions, basal cells were cultured on pre-coated plates with laminin-enriched 804G cell-conditioned medium (804G-CM) and placed at 37 ºC in humidified air with 5% CO_2. When cells reached 50 to 70% confluence, they were dissociated with conventional trypsinization and either split at a 1:10 ratio or utilized for gene editing and *in vitro* differentiation. The 804G cell line, a rat bladder epithelial cell line kindly provided by Dr. Hongmei Mou (Massachusetts General Hospital, Boston, MA, USA), was cultured in RPMI-1640 (Sigma Aldrich, St. Louis, MO) supplemented with 10 % Fetal Bovine Serum (FBS) (GE healthcare, Chicago, IL) and 1 % Penicillin-Streptomycin (pen-strep) (Thermo Fisher Scientific, Waltham, MA). Once cells reached confluence in a 225 cm^2 culture flask (Corning, Corning, NY), culture supernatant was replaced with 100 ml fresh medium, and collected every other day for up to 3 collections. All media obtained were filter-sterilized and stored at 4 ºC. Both basal cells and 804G cells were cryo-preserved in CryoStor® CS10 (STEMCELL Technologies) and kept frozen in liquid N_2.

Characterization of airway basal cells: Airway basal cells were analyzed with cell surface markers CD49f and NGFR using flow cytometric analysis. Briefly, dissociated cells were stained with α-CD49f-PE (Biolegend, San Diego, CA) and/or α-CD271(NGFR)-APC (Biolegend) on ice for 30min. Non-immune IgG2a-PE and IgG1, as well as κ-APC were used as isotype controls. Antibody-stained cells were washed with FACS buffer (phosphate buffered saline with 1 % FBS), pelleted by a 5-minute centrifugation at 200g and then re-suspended with FACS buffer containing 0.075 µg/ml 4',6-diamidino-2-phenylindole (DAPI) (Thermo Fisher Scientific) for live cell separation. Stained cells were analyzed on a FACS LSRII (BD Biosciences, San Jose, CA) using FACS Diva software (BD Biosciences).

***In vitro* differentiation of basal cells at air liquid interface (ALI):** 200,000 airway basal cells in Pneumacult™-Ex Plus medium were seeded on the top chamber of a 6.5 mm Transwell® with 0.4 µm pore polyester membrane inserts (Corning) pre-coated with 804G-CM. Initially, medium was added to both the top and bottom chambers. The medium was replaced the following day by Pneumacult-ALI medium (STEMCELL Technologies). After an additional day, medium from the top chamber was removed to establish the ALI and cells were maintained, with daily feeding, in this manner for approximately 4 weeks.

Histological and immunofluorescence analysis: Well-differentiated airway epithelia at ALI were fixed at 4°C overnight in 4 % paraformaldehyde (PFA) (Electron Microscopy Sciences, Hatfield, PA). Fixed samples were dehydrated with a series of increasing concentrations of ethanol, cleared with xylene and infiltrated with paraffin before embedding in wax. Sections of 5 µm thickness were transversely cut using an HM 325 Rotary Microtome (Thermo Fisher Scientific), followed by staining with haematoxylin and eosin. For immunofluorescence analysis, fixed cells were immunostained on transwell inserts to perform whole mount staining, or cryo-sectioned transversely to image airway epithelium. Cryo-section samples were prepared following sequential sucrose treatment (15 %, then 30 % sucrose), flash freezing in OCT embedding medium (Thermo Fisher Scientific), and sectioning (5-8 µm thickness) using a Leica® CM1850 Cryostat (Leica Biosystems Inc., Buffalo Grove, IL). Whole inserts and sectioned samples were stained with primary/secondary antibodies listed in **Table S5** utilizing standard immunofluorescence procedures. Briefly, samples were permeabilized with 0.3 % Triton X-100 (Sigma) in PBS for 15-30 min and blocked with 2 % bovine serum albumin (BSA) for 1 hour. Samples were then incubated with primary antibodies in 2 % BSA overnight at 4 ºC, followed by the incubation with the respective secondary antibodies in 2 % BSA at room temperature for one to two hours. Three 5 minute washes in PBS were performed after each antibody treatment. Prolong™ Gold Antifade Mountant with DAPI (Thermo Fisher Scientific) was added to counter-stain. Samples were then mounted and cured for 24 hours prior to imaging. Images were acquired using a Leica DMi8 microscope (Leica Microsystems, Wetzlar, Germany) and Leica Application Suite Software (Leica

Microsystems). Quantification of each epithelial cell type was performed by counting the number of cells staining for specific markers in three random 40x magnification fields. The frequency of each cell type was calculated relative to the total number of cells as determined by DAPI stained nuclei (approximately 450 cells total from three random fields). Statistical calculations in Figure S3 were performed using GraphPad Prism® v8.2.1 (GraphPad Software, San Diego, CA) and statistical significance was determined using Two-tailed paired t-test compared to control with 95% confidence interval.

Gene editing reagents: Zinc Finger Nucleases (ZFNs) targeting intron 7, intron 8, or the ΔF508 mutant sequence of human *CFTR* were subcloned into individual vectors (pVAX-GEM) containing a T7 RNA polymerase promoter, a 5' UTR sequence derived from the Xenopus beta-globin gene, a 3' UTR containing the Woodchuck Hepatitis Virus Response Element (WPRE) sequence, and polyA tract. ZFN mRNAs were synthesized *in vitro* either commercially (TriLink BioTechnologies, San Diego, CA) with ARCA Cap modification or in house using the mMESSAGE mMACHINE T7 Ultra kit followed by the purification with a MEGAclear kit (Thermo Fisher Scientific).

An approximately 2 kb *wtCFTR* AAV-6 donor spanning exon 11 was prepared by PCR amplification of *wtCFTR* (1963bp) from DD023J (non-CF) genomic DNA utilizing PCR primers CFaav2kb Fw and R, cloning into an AAV-2 ITR-containing plasmid backbone (pAAV2-MCS; Cell Biolabs, San Diego, CA), and produced commercially (Vigene Biosciences, Inc., Rockville, MD). The partial *CFTR* cDNA intron 7 and intron 8 donor constructs contained a codon-optimized human partial *CFTR* cDNA, a splice acceptor sequence derived from human FIX, and the bovine growth hormone (bGH) poly adenylation sequence. These constructs, denoted *SA-CFTR*$_{8\text{-}27}$*-pA* and *SA-CFTR*$_{9\text{-}27}$*-pA*, were flanked by homology sequences of approximately 500-600 bp in total length from human *CFTR* introns 7 and 8, respectively. To simultaneously measure gene disruption (indels) and homology directed repair (HDR)-mediated TI alleles, AAV donor constructs also included a primer binding site (green arrows in **Figure 3A** for intron 8 targeting) followed by a TI-specific barcode (gray box in **Figure 3A** for intron 8 targeting) just upstream of the right homology arm. Recombinant AAV-2/6 vectors (comprised of AAV-2 ITRs and the AAV-6 capsid) carrying intron 7 and intron 8 partial *CFTR* cDNA donors were produced by triple transfection of HEK293 cells in 10-chamber CELLSTACK culture chambers (Corning), and purified by cesium chloride density gradient centrifugation followed by dialysis. Viral genome concentrations were measured by quantitative polymerase chain reaction (qPCR). The 200-mer single strand oligo DNA donor (ssDNA) was synthesized by Integrated DNA Technologies (IDT) (Coralville, IA). All donor DNA sequences are shown above (Donor DNA sequences).

Gene editing: Trypsin-dissociated airway basal cells were resuspended in 100µl BTXpress™ solution (Harvard Apparatus, Holliston, MA) with ZFN mRNAs and electroporated in BTX™ electroporation cuvettes (2mm gap, Harvard Apparatus) under Low Voltage (LV) conditions of 250 V for 5 ms, and 1 pulse using BTX™ ECM 830 electroporation generator (Harvard Apparatus). The number of cells (2–5 x 10^5 cells per reaction) and ZFN mRNA amount (typically 2-3 ug of each ZFN-L and ZFN-R mRNA per reaction) were optimized for each targeting site and strategy. The electroporated cell/ZFN mRNA solution was transferred into a 1.5 ml tube and immediately transduced with AAV-6 donor at a multiplicity of infection (MOI) optimized for each targeting site (typically 1-6 x10^6 viral genomes per cell (vg/cell)) for 20 min. Cells, together with AAV-6 donor, were cultured overnight in Pneumacult™-Ex Plus medium on 804G CM-coated plates. Alternatively, sequence-specific correction of ΔF508 mutation with ssDNA donor was performed via co-electoroporation of 2 µg each ZFN11 mRNA together with 10 - 30 µg of 200-mer ssDNA donor. Co-electroporated cells were immediately plated in Pneumacult™-Ex Plus medium on 804G-CM-coated plates.

Assessment of on-target genome modification: Induction of on-target indels, sequence-specific correction, and targeted integration were assessed quantitatively through NGS deep sequencing on an Illumina platform. For assessing ZFN11-induced indels and ΔF508 correction, genomic DNA (gDNA) from gene-edited cells was first PCR-amplified using primers CFi10aFw and CFi11aRv indicated as f_1 and r_2 in **Figure 2A**, respectively, in order to avoid sequencing of residual ssDNA oligo or episomal AAV-6 donor DNAs. Nested PCR amplification was subsequently performed using primers Ex11 Miseq-Fw and -Rv to prepare ~ 200 bp amplicons for paired-end deep sequencing on an Illumina MiSeq sequencer (Illumina, San Diego, CA).

In order to permit simultaneous NGS-mediated assessment of gene disruption (indels) and HDR-mediated TI alleles for the targeting of introns 7 and 8, AAV donor constructs also included a primer binding site followed by a TI-specific barcode just upstream of the right homology arm (highlighted in **Figure 3A** for intron 8 targeting, for example). Once amplified with a reverse primer (black arrows in **Figure 3A** for intron 8 targeting) which binds just downstream of the right homology arm within the genome, both wildtype and modified (indels and HDR-mediated TI) alleles were amplified simultaneously, and frequencies of each mode of gene modification were assessed via paired-end MiSeq sequencing. The system was designed such that no PCR bias occurs with amplification of the TI alleles vs. wildtype alleles since the PCR amplicon was the same length and base composition. Examples of sequencing data are uploaded in supplementary files (Intron 8 NGS.xlsx, Intron 7 NGS.xlsx). One TI-8 experiment in ΔF508/ΔF508 cells, showing extremely low frequency of indels as well as TI-8, was excluded from further analysis and presentation – due to concern that the electroporation step on this occasion was not successful.

In some cases, as in **Figure S2**, sequence-specific correction of ΔF508 mutation was also assessed by the web based bioinformatics tool "Tracking of Insertions, DEletions and Recombination events" (TIDER) (https://tider.deskgen.com/) [1]. Briefly, genomic DNA from edited cells was amplified by PCR with primers CFi10aFw and CFi11aRv and Sanger sequenced with primer CF5 followed by TIDER analysis. The 'guide sequence' for the TIDER analysis was 5'- AATATCATTGGTGTTTCCTA-3'; control and reference chromatogram for the analyses were sequences from genomic DNA of KK003K (Δ*F508/*Δ*F508 CFTR)* and DD023J (non-CF), respectively. TI-8 was also assessed semi-quantitatively by PCR amplification of genomic DNA from edited cells with primers CF34f and CF35r, followed by digestion with Eco RI (**Figure S5B**). TI-7 was similarly analyzed by PCR amplification with primers CF36f and CF37r, followed by Eco RI digestion. Digested and undigested PCR product were resolved with a 3 % agarose gel.

Southern blot analysis of edited cells: 20µg of genomic DNAs (gDNAs) isolated with GentraPura gene Core A (Qiagen, Hilden, Germany) were digested overnight with Eco RI and purified by ethanol precipitation. The gDNAs were then resolved on 0.7 % agarose gel, transferred to a Nytran Super Charge membrane (GE Healthcare), and hybridized with [^{32}P]-labeled probe. As probe, a 246 bp *CFTR* exon 8 fragment was synthesized (IDT) and labeled with [^{32}P]dCTP using Prime-It II Random Primer Labeling kit (Agilent Technologies, Santa Clara, CA). Following hybridization, the membrane was washed, exposed to X-ray film, and scanned.

***CFTR* RT-PCR:** Total RNA was isolated from ALI culture with the Nucleospin RNA XS kit (Macherey-Nagel Inc, Bethlehem, PA). cDNA synthesis was performed with the Improm-II Reverse Transcriptase oligo dT kit (Promega, Madison, WI) and RT-PCR were performed with Gotaq Hot Start polymerase (Promega). TI-8 cDNA samples were analyzed with PCR primer pairs 72CF-wt8f and 81CF-wt9r for the endogenous transcript and with primers 72CF-wt8f and 81CF-opt9r for the chimeric endogenous-transgene transcript. TI-7 cDNA samples were analyzed with primers 70CF-wt7f and 81CF-wt9r for the endogenous transcript and with primers 70CF-wt7f and 81CF-opt9r for the chimeric endogenous-trangene transcript.

Western blot analysis of CFTR protein: After thorough washing with PBS, ALI cultured cells were lysed with RIPA Lysis and Extraction Buffer (Thermo Fisher Scientific). Lysate was twice flash frozen and thawed, and centrifuged at 3000 x g for 10 min (4 ºC) to obtain protein extracts. Sixty µg of protein was brought to a volume of 50 µl with RIPA buffer, sample reducing agent (Thermo Fisher Scientific), and sample buffer (Thermo Fisher Scientific). Proteins were resolved by electrophoresis through a NuPAGE 7 % Tris-Acetate Protein Gel using SDS-PAGE methodology, transferred onto Hybond-C nitrocellulose transfer membrane (GE Healthcare), and blocked with 5 % non-fat dry milk in PBS (blocking buffer) at room temperature for 30 minutes. The blot membrane was incubated in blocking buffer overnight at 4 ºC with anti-CFTR primary antibody A4 596 (Cystic Fibrosis Foundation Therapeutics), followed by 4 washing steps for 5 minutes each in 1xTBS containing 0.1 % Tween 20 and 0.25 % non-fat dry milk (washing buffer). Subsequently, the membrane was incubated for 1 hour at 4 ºC in in blocking buffer containing HRP-linked horse anti-mouse secondary antibody (Cell Signaling Technologies, Danvers, MA), followed by washing 4 times with washing buffer and chemiluminescent detection using Amersham

ECL Prime (GE Healthcare). As loading control, calnexin was probed and detected with anti-Calnexin polyclonal antibody (Abcam, Cambridge, United Kingdom) followed by secondary HRP goat anti rabbit IgG (Abcam).

Ussing chamber analysis: Ussing chamber experiments were performed on EasyMount Ussing Chamber Systems at voltage clamp mode, and Acquire & Analyze software (Physiologic Instruments) was employed to record and analyze data. Briefly, transwell inserts were mounted into chambers and bathed in low chloride Ringer`s solution (1.2 mM NaCl, 140 mM Na-gluconate, 25 mM $NaHCO_3$, 3.33 mM KH_2PO_4, 0.83 mM K_2HPO_4, 1.2mM $CaCl_2$, 1.2 mM $MgCl_2$, 10 mM glucose) at apical and Ringer's solution (120 mM NaCl, 25 mM $NaHCO_3$, 3.33 mM KH_2PO_4, 0.83 mM K_2HPO_4, 1.2mM $CaCl_2$, 1.2 mM $MgCl_2$, 10 mM glucose) at basolateral side of monolayer. After base line is stabilized, 100 µM amiloride (Sigma) applied to both sides of the chamber to carry out complete inhibition of ENaC (Epithelial sodium channel). Subsequently, 10 µM forskolin (Sigma) were administered to stimulate chloride current. At the end of experiments, 10 µM CFTR inhibitor-172 (Sigma) employed at the apical side to specifically inhibit CFTR function following by 100 µM UTP at the apical side to asses the integrity of developed epithelium. The resulting change in short circuit current was calculated as ΔI_{sc}. For some samples, ALI-cultured cells were pre-treated with 3 µM VX-809 and 1 µM VX-770 for 48 hour prior to Ussing chamber analysis to modulate CFTR expression and function. The data were expressed in mean±SD.

Clonal isolation of TI-8 cells: Single cell-derived clones were isolated from bulk TI-8 treated cells via limiting dilution utilizing a modified conditionally reprogrammed cell (CRC) method[3, 4]. Briefly, bulk edited cells were dissociated with trypsin into single cells and diluted in CRC medium consisting of a 3:1(v/v) mixture of complete DMEM medium (DMEM high glucose containing 10% FBS, 2mM L-glutamine and 100U/ml Penicillin-Streptomycin) (Gibco) and F-12 Nutrient Mix (Gibco), 25 ng/ml hydrocortisone (Sigma), 0.125 ng/ml EGF (Invitrogen), 5 µg/ml insulin (Sigma), 250 ng/ml fungizone/amphotericin B (Fisher), 10 µg/ml Gentamicin (Gibco), 0.1 nM cholera toxin (Sigma) and 10 µM Y-27362 (Reagents Direct) and then plated by limiting dilution onto a feeder layer of irradiated NIH3T3 cells in a 96 well plate. Each well was monitored via inverted light microscopy for the appearance of a single colony per well. Each colony was further expanded in SMAD inhibition medium or in PneumaCult™ ExPlus medium.

Quantification of TI-8 mRNA transcript composition: Quantitative RT-PCR was performed on RNA isolated from single-cell derived clones of TI-8 edited airway basal cells that had been cultured under ALI conditions for 3 - 4 weeks. Quantitative RT-PCR was performed using the PowerUp™ SYBR™ Green Master Mix (Applied Biosystems, CA) on a 7900HT Fast Real-Time PCR System (Applied Biosystems). The endogenous *CFTR* transcript was amplified with primer pair: WTex8 qPCRf (E8 in **Figure S8D**) and WTex9-10 qPCRr (E9-10 in **Figure S8D**). The chimeric endogenous-transgenic *CFTR* transcript was detected with the primer pair: WTex8 qPCRf (E8) and optex9-10 qPCRr (T9-10 in **Figure S8D**). The standard curve for absolute quantification of *CFTR* transcript copy number was obtaind from serial diliution of a 250 bp double stranded, synthesized DNA that contained either the endogenous exons 8, 9 and 10 or the endogenous exon 8 directly joined to codon optimized transgenic exons 9 and 10.

Assessment of ZFN8 off-target genome modification and ZFN8 optimization: The lead h*CFTR* intron 8 - targeted ZFN pair was subjected to unbiased identification of candidate off-target sites using methods similar to those previously described[5]. Briefly, K562 cells were electroporated with mRNA encoding the ZFNs as well as barcoded DNA oligonucleotides using the BTX ECM 830 electroporator to allow for unbiased identification of sites which had undergone double-stranded DNA cleavage and NHEJ-mediated integration of the DNA oligonucleotides. The top 32 loci containing integrated oligonucleotides was then subjected to a validation procedure in primary human basal airway epithelial cells. For each off-target site (designated "OT2" through "OT32"), an oligonucleotide primer pair was designed that enabled amplification of a 120-200 base pair (bp) fragment. Primers were also similarly designed for the intended target in *CFTR* (designated "OT1"). Primers designed against target loci were then screened for predicted amplification specificity by a genome-wide *in silico* PCR simulation. Optimal primer pairs emerging from this step were extended via appending of adapter sequences necessary for a second "barcode"

PCR to attach priming sites and barcodes for the MiSeq process. The ZFN design was optimized as described [6] in order to reduce the incidence of off-target indels, while still retaining recognition of the same intron 8 target sequence.

REFERENCES

1. Brinkman, EK, Kousholt, AN, Harmsen, T, Leemans, C, Chen, T, Jonkers, J, and van Steensel, B (2018). Easy quantification of template-directed crispr/cas9 editing. Nucleic Acids Res *46*, e58.
2. Mou, H, Vinarsky, V, Tata, PR, Brazauskas, K, Choi, SH, Crooke, AK, Zhang, B, Solomon, GM, Turner, B, Bihler, H, et al. (2016). Dual smad signaling inhibition enables long-term expansion of diverse epithelial basal cells. Cell Stem Cell *19*, 217-231.
3. Ghosh, M, Ahmad, S, White, CW, and Reynolds, SD (2017). Transplantation of airway epithelial stem/progenitor cells: A future for cell-based therapy. Am J Respir Cell Mol Biol *56*, 1-10.
4. Hayes, D, Jr., Kopp, BT, Hill, CL, Lallier, SW, Schwartz, CM, Tadesse, M, Alsudayri, A, and Reynolds, SD (2019). Cell therapy for cystic fibrosis lung disease: Regenerative basal cell amplification. Stem Cells Transl Med *8*, 225-235.
5. Tsai, SQ, Zheng, Z, Nguyen, NT, Liebers, M, Topkar, VV, Thapar, V, Wyvekens, N, Khayter, C, Iafrate, AJ, Le, LP, et al. (2015). Guide-seq enables genome-wide profiling of off-target cleavage by crispr-cas nucleases. Nat Biotechnol *33*, 187-197.
6. Miller, JC, Patil, DP, Xia, DF, Paine, CB, Fauser, F, Richards, HW, Shivak, DA, Bendana, YR, Hinkley, SJ, Scarlott, NA, et al. (2019). Enhancing gene editing specificity by attenuating DNA cleavage kinetics. Nat Biotechnol *37*, 945-952.